

Understanding the Dynamics of Amebiasis Using Mathematical Modelling Approach: Optimal Control Strategies and Cost-Effectiveness Analysis

K. A. Tijani ^{1*}, C. E. Madubueze ¹

- 1. Department of Mathematics, Joseph Sarwuan Tarka University formerly Federal University of Agriculture, Makurdi, Benue State, Nigeria.
- * Corresponding author: kazeemtijani1987@yahoo.com¹

Article Info

Received: 01 September 2025 Revised: 09 October 2025

Accepted: 11 October 2025 Available online: 15 October 2025

Abstract

Amebiasis is a parasitic infection of the intestine caused by the amoeba Entamoeba histolytica, and it is endemic in tropical countries with poor sanitation and hygiene practices. To explore the dynamics of amebiasis and identify effective control interventions, a mathematical model is developed. This model incorporates a treatment class within the human population and accounts for the concentration of the amebiasis pathogen in the environment. The study derived the steady states, stability, and the basic reproduction number of the infection. A global sensitivity analysis is also conducted to identify the most significant parameters influencing the disease's spread. Subsequently, an optimal control model is formulated, featuring four time-dependent controls: hygiene practices, efficient screening of infected individuals, effective treatment, and disinfection/sterilisation of the environment. This model is analysed and simulated across four categories — single, double, triple, and quadruple combination cases — to assess the impact of these control measures. Additionally, a cost-effectiveness analysis is conducted using the incremental cost-effectiveness ratio (ICER) method. The findings offer valuable insights that can help policymakers effectively control the disease while managing limited resources. The results indicate that any control combination that includes efficient screening of infected individuals is the most cost-effective strategy for reducing amebiasis in society. However, in a single case where resources are limited, Strategy 2 - efficient screening of infected individuals - emerges as the most cost-effective method for eradicating the disease. With additional resources, the most effective double-combined control strategy for disease eradication is Strategy 8, which combines Strategy 2 with efficient treatment. For the triple control strategy, the most cost-effective control Strategy is Strategy 14, which integrates Strategy 8 and disinfection/sterilisation of the environment. However, the overall most cost-effective strategy remains Strategy 2.

Keywords: Amebiasis, Mathematical model, Global sensitivity analysis, Optimal control, Cost-effectiveness analysis.

MSC2010: 00A71, 93A30.



International Journal of Mathematical Sciences and Optimization: Theory and Applications 11(3), 2025, Pages 138 - 166

HTTPS://DOI.ORG/10.5281/ZENODO.17604865

1 Introduction

Amebiasis is common in tropical countries with poor sanitation and hygiene practices [1,2]. It is endemic in developing countries of the Indian subcontinent, parts of Central and South America, Mexico, Asia, and certain parts of Africa [3,4]. It has become a public health challenge [5]. About 50 million people across the globe develop an amebiasis infection each year, and about 0.1 million people die of this disease yearly [4].

Amebiasis is known to be a parasitic infection of the intestine caused by the amoeba *Entamoeba* histolytica or E. histolytica. E. histolytica is a single-celled protozoan that usually enters the human body when a susceptible individual ingests cysts through food or water [2,6]. It can also enter the body through direct contact with faecal-oral means [3,4]. It can also be transmitted during anal sex, and oral sex [1,5]. The cysts are a relatively inactive form of the parasite that can live for several months in the soil or environment where they were deposited in faeces [6,7].

Only about 10% to 20% of people infected with *E. histolytica* become ill [5,6]. The symptoms are mostly mild, which include diarrhoea, stomach pain and stomach cramping. Symptoms usually appear (incubation period) within 2 to 4 weeks, but can develop later [4]. After the incubation period, the infected individual may develop either an asymptomatic stage or an acute stage of amebiasis colitis [7,8]. In a rare complication of amebiasis, it can enter the bloodstream, and go through various internal organs, which mostly can end up in the liver, but can also infect the heart, brain or other organs [2,3].

If this disease invades the internal organ, it tends to cause severe illness and death, potentially [1]. The mortality rates of dysenteric syndrome due to E. histolytica are less than 1% but the mortality due to its complications rises to 75% [7].

Certain precautions can be taken to prevent amebiasis, even though there is no vaccine against the disease presently. These precautions include proper sanitation, thorough hand washing with soap and water after using the toilet and before handling food. Additionally, when travelling to areas where the disease is endemic, hygiene practices should be observed at all times [2, 3, 7]. Following a diagnosis, the disease can be treated with antibiotics. However, if left untreated, it may become fatal. [4].

The mathematical modelling of infectious diseases is an essential tool for analysing the dynamic nature of infectious diseases. It helps develop control strategies to forecast appropriate control strategies [9]. While an optimal control problem requires regularising and solving problems by choosing the best way in a dynamic process, which depends on controls and is always subject to constraints [25]. This was employed by [11, 15, 38] among others. Meanwhile, Cost-effectiveness analysis (CEA) is a type of economic evaluation and assessment focused on efficiency to maximise the value of available resources, or, precisely, the value of money [26] as used by [12, 21, 24, 39].

Many authors have utilised the concept of mathematical modelling to analyse the dynamics of infectious diseases, such as [9] and [10], who employed mathematical modelling to study COVID-19, and [11], who investigated the dynamics of the Zika virus using this approach. Relatedly, [12] used the same concept to investigate the dynamics of typhoid fever.

Few authors have worked on amebiasis using the concept of mathematical modelling, among them are: [14–19]. Although they produced some useful results, [14] examined the *SEICR* model, whose findings suggest that infection propagation must reach a steady state, allowing for the evaluation of the extent and depth of the infection in a reasonable manner. However, they did not take into account the treated compartment or the disease concentration in the environment. Additionally, they did not consider optimal control or cost-effectiveness analysis, which are essential for determining the most cost-effective strategies, particularly in developing countries where resources are limited and the disease is endemic.

Also, [15] studied SEICR model with incorporation of amebiasis pathogen compartment, B. Their results show that for single control, an awareness program should be considered, while for double control, an awareness program and treatment are the most effective strategies for eliminating the disease. They concluded that the most effective approach to eliminating the disease is a



International Journal of Mathematical Sciences and Optimization: Theory and Applications 11(3), 2025, Pages 138 - 166

HTTPS://DOI.ORG/10.5281/ZENODO.17604865

combination of these three controls, forming a triple control. However, they did not consider the treatment compartment or the cost-effectiveness analysis, which would help determine the most cost-effective strategy, especially in limited-resource countries where the disease is endemic.

Mpeshe [16] worked on *SEIR* model and their outcome revealed that personal prevention and hygiene practices will help to reduce the number of cysts ingestion and as well reduce the transmission rate. They failed to consider the treated compartment, as well as the disease pathogen concentration class, which is the primary means of contracting the disease. They did not account for this in their force of infection, nor did they consider global sensitivity analysis, optimal control, and cost-effectiveness analysis in their work.

[17] also formulated SEICR with the pathogen compartment, and their results show that indirect transmission has a greater influence on the spread of the disease, while screening, treatment, and sanitation can significantly reduce its spread. However, they did not consider the treatment compartment, nor did they perform global sensitivity analysis in their work. They also failed to consider optimal control and cost-effectiveness analysis in their study.

[18] analysed the *SEICR* model for amebiasis dynamics, highlighting issues with the existence and uniqueness of the Initial Value Problem (IVP) solutions under certain parameter conditions. Their work overlooked the treatment compartment, the amebiasis pathogen class, global sensitivity analysis, and the endemic equilibrium state. Additionally, optimal control and cost-effectiveness analysis were not addressed.

Mwaijande and Mpogolo [19] studied SEICR in relation to the amebiasis pathogen and found that carriers significantly impact the prevalence of amoebiasis, and ignoring them hampers containment efforts. However, they did not include a treatment compartment or conduct global sensitivity analysis, optimal control, and cost-effectiveness analysis, which are crucial for determining cost-effective strategies in resource-limited, endemic regions.

This study aims to investigate the dynamics of amebiasis by incorporating a treatment compartment, the amebiasis pathogen compartment, and examining both direct and indirect transmission modes, providing cost-effective optimal control interventions. This is to prevent infected individuals, through treatment, from shedding and spreading the disease in the population, and also cut off the means of transmission from the environment [1, 3]. A six-compartmental deterministic model will be developed, including: Susceptible human population, $S_h(t)$; Latent human population, $L_h(t)$; Infected human population, $I_h(t)$; Treated human population, $I_h(t)$; Recovered human population, $R_h(t)$; and amebiasis pathogen concentration in the environment, $P_c(t)$.

The paper is organised as follows: Section 2 presents the model formulation and mathematical analysis of the amebiasis model. Section 3 includes results from global sensitivity analysis using Latin Hypercube sampling (LHS) and optimal control analysis. Section 4 discusses numerical simulations and cost-effectiveness analysis. Section 5 concludes with an overview of the research findings. This initiative aims to protect individuals who are at high risk of exposure to the disease due to to their occupations and to analyse the effects of treatment on infected humans

2 Model formulation

We develop a non-linear mathematical model to study the dynamics of amebiasis, incorporating a treatment compartment and pathogen compartment, along with both direct and indirect transmission modes. The human population is divided into five compartments at time t: Susceptible $S_h(t)$, Latent $L_h(t)$, Infected $I_h(t)$, Treatment $T_h(t)$, and Recovered $R_h(t)$, where $N(t) = S_h(t) + L_h(t) + I_h(t) + T_h(t) + R_h(t)$. The model also considers the pathogen concentration in the environment $P_c(t)$. The following assumptions have been considered:

- It is assumed that the total human population in a given society is homogeneous at all times [2,3].
- It is assumed that people in the treatment class (infected individuals undergoing treatment) can also spread the disease, as they are not confined to a restricted place [3]. Although





HTTPS://DOI.ORG/10.5281/ZENODO.17604865

they are aware of having the disease, the rate of contracting it from such individuals might be minimal because some of them may be more conscious, which prompts the idea of the modification parameter α .

• It is assumed that people can die of the disease in both $I_h(t)$ and $T_h(t)$ [1, 5, 6].

In the model, births and immigration are added to the susceptible human population, $S_h(t)$, at the rate of Λ_h , and this population also increases at the rate of γ due to the recovery class from loss of immunity. [3, 7]. Individuals in the compartment $S_h(t)$ can contract the disease at a rate λ , transitioning to the pre-infected or latent state $L_h(t)$. The force of infection is defined by the equation $\lambda = |\beta_1(I_h + \alpha T_h) + \beta_2 P_c|$. In this equation, β_1 represents the transmission rate from human to human, α is the modification parameter for individuals receiving treatment, and β_2 is the transmission rate from the environment to humans [1, 2, 4].

Individuals in the L_h compartment decrease at a rate of σ and subsequently progress to the infected class I_h after the incubation period [1].

The population of individuals in the infected class, denoted as I_h , decreases due to disease-induced mortality, represented by the rate d_1 , as well as from the screening rate τ . This population then progresses to the treated class, T_h [3]. Meanwhile, the population of T_h declines due to diseaseinduced mortality at the rate d_2 and as a result of the treatment rate η , which allows individuals to progress to the recovered class, R_h [6]. Additionally, μ_h represents the natural death rate of the human population.

The concentration of pathogens in the environment increases due to shedding from both the infected class, I_h , and the treated class, T_h , at rates π_1 and π_2 respectively [2]. Furthermore, the concentration of pathogens decreases due to the natural decay rate, μ_c [3].

A graphical representation of the model formulation is shown in Figure 1, while the state variables and parameter descriptions are detailed in Table 1.

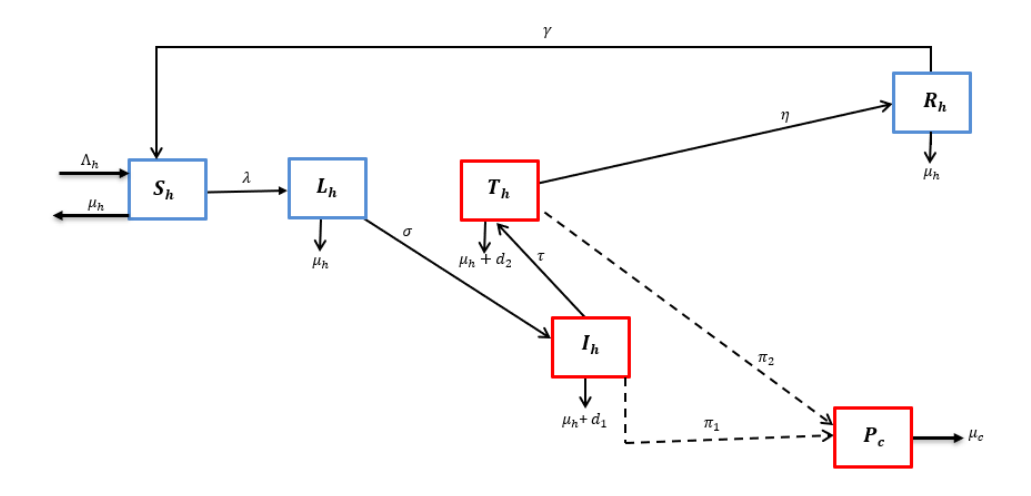


Figure 1: Systematic Diagram of the Amebiasis Model.

The following system of non-linear differential equations is formulated based on the assumptions of the model, the parameters in Table 1 and Table 2, respectively, while the flow diagram is shown in Figure 1 with the corresponding system of equations in (2.1):



Table 1: State Variables of the Model			
State Variable	Epidemiological Interpretation	${f Unit}$	
$S_h(t)$	Susceptible human population per time, t	Human population	
$L_h(t)$	Latent(pre-infectious) human population per time, t	Human population	
$I_h(t)$	Infected human population per time, t	Human population	
$T_h(t)$	Human population undergoing treatment per time, t	Human population	
$R_h(t)$	Recovered human population per time, t	Human population	
$P_c(t)$	Amebiasis pathogen concentration in the environment per time, t	Pathogen concentration	

$$\frac{dS_h}{dt} = \Lambda_h - \lambda S_h + \gamma R_h - \mu_h S_h,$$

$$\frac{dL_h}{dt} = \lambda S_h - (\sigma + \mu_h) L_h,$$

$$\frac{dI_h}{dt} = \sigma L_h - (\tau + d_1 + \mu_h) I_h,$$

$$\frac{dT_h}{dt} = \tau I_h - (\eta + d_2 + \mu_h) T_h,$$

$$\frac{dR_h}{dt} = \eta T_h - (\gamma + \mu_h) R_h,$$

$$\frac{dP_c}{dt} = \pi_1 I_h + \pi_2 T_h - \mu_c P_c,$$
(2.1)

with non-negative initial conditions, $S_h(0)$, $L_h(0)$, $I_h(0)$, $I_h(0)$, $R_h(0)$, and $P_c(0)$, where $\lambda = [\beta_1(I_h + \alpha T_h) + \beta_2 P_c]$.

The model parameters are assumed to be non-negative except for human recruitment, which is strictly positive.

Table 2: Description and parameter values of the model

Parameter	Description	Unit	Value	Source
Λ_h	Human recruitment rate	Human population year	6	Estimated
β_1	Human-to-human transmission rate	$year^{-1}$	0.0000165	Assumed
eta_2	Environment-to-human transmission rate	$year^{-1}$	0.001223	[23]
σ	Progress rate from L_h to I_h after latent period	$year^{-1}$	0.0714	[7, 27]
α	Modification parameter for T_h contact rate	Dimensionless	0.02	Assumed
μ_h	Human natural death rate	$year^{-1}$	0.0000548	[29]
d_1	Disease induced death rate by I_h	$year^{-1}$	0.000137	[15]
d_2	Disease induced death rate by T_h	$year^{-1}$	0.000219	Estimated
η	Recovery rate due to treatment	$year^{-1}$	0.0714	[16, 30]
γ	Progress rate from R_h to S_h due to loss of immunity	$redyear^{-1}$	0.09	Assumed
au	Progress rate from I_h to T_h	$year^{-1}$	0.4	Assumed
π_1	Shedding rate from I_h to P_c	$year^{-1}$	0.07	Assumed
π_2	Shedding rate from T_h to P_c	$year^{-1}$	0.04	Assumed
μ_c	Natural pathogen decay rate	$year^{-1}$	0.83	[15]

2.1 Invariant region

This region will be determined by applying the following theorem.

Theorem 2.1. The solution of the system is feasible for all t > 0 if they enter the invariant region $\Pi = \Pi_1 \times \Pi_2$ such that

$$\Pi_{2} = \left\{ (S_{h}, L_{h}, I_{h}, T_{h}, R_{h}) \in \Re_{+}^{5}, : S_{h}(0) > 0, L_{h}(0) \ge 0, I_{h}(0) > 0, T_{h}(0) \text{ and } R(0) \ge 0, N \le \frac{\Lambda_{h}}{\mu_{h}} \right\}$$
and
$$\Pi_{2} = \left\{ P_{c} \in \Re_{+}^{1}, : P_{c}(0) \ge 0 P_{c} \le \frac{\Lambda_{h}(\pi_{1} + \pi_{2})}{\mu_{h}\mu_{c}} \right\}.$$



As adopted by Tijani et al [13], Odeh et al. [11] and Mpeshe [16], The total population is defined as $N(t) = S_h(t) + L_h(t) + I_h(t) + T_h(t) + R_h(t)$, giving

$$\frac{dN}{dt} = \Lambda_h - d_1 I_h - d_2 T_h - \mu_h N. \tag{2.2}$$

In the absence of disease-induced death i.e. $d_1 = d_2 = 0$, the Equation (2.2) becomes.

$$\frac{dN}{dt} \le \Lambda_h - \mu_h N. \tag{2.3}$$

Solving the differential inequality (2.3) by finding the integrating factor (I.F), we have I.F = $e^{(\int \mu_h t dt)}$. Thus,

$$\frac{d}{dt}(Ne^{(\mu_h t)}) \le \Lambda_h e^{(\mu_h t)}.$$

Integration on each side gives

$$(Ne^{(\mu_h t)}) \le \frac{\Lambda_h}{\mu_h} e^{(\mu_h t)} + A.$$

where A is the constant of integration. Therefore,

$$N(t) \le \frac{\Lambda_h}{\mu_h} + Ae^{(-\mu_h t)}. \tag{2.4}$$

Applying the initial condition at t = 0 that is $N(0) = N_0$ in Equation (2.5), we have

$$N \leq \frac{\Lambda_h}{\mu_h} + (N_0 - \frac{\Lambda_h}{\mu_h})e^{(-\mu_h t)}.$$

Thus, applying the differential inequality by [20], then $0 \le N \le \frac{\Lambda}{\mu}$ as $t \to \infty$. Therefore, the feasible solutions of the human population of the model (2.1) enter the region

$$\Pi_1 = \left\{ (S_h, L_h, I_h, T_h, R_h) \in \Re_+^5, : S_h(0) > 0, L_h(0) \ge 0, I_h(0) > 0, T_h(0) \text{ and } R(0) \ge 0, N \le \frac{\Lambda_h}{\mu_h} \right\}$$

This implies that every solution with initial conditions in Π_1 remains in the region for t > 0. Therefore the region Π_1 is positively invariant. Also, considering the pathogen concentration class and the last equation of system (2.1) as in the work of [21], we have

$$\frac{dP_c}{dt} = \pi_1 I_h + \pi_2 T_h - \mu_c P_c \le (\pi_1 + \pi_2) \frac{\Lambda_h}{\mu_h} - \mu_c P_c, \tag{2.5}$$

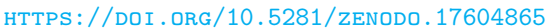
since $N(t) \leq \frac{\Lambda_h}{\mu_h}$ and $I_h \leq \frac{\Lambda_h}{\mu_h}$ and $T_h \leq \frac{\Lambda_h}{\mu_h}$. Employing the method of integrating factor to Equation (2.5) and solving with the initial condition, $P_c(0) = P_{c0}$ yields

$$\frac{dP_c}{dt} \le \frac{(\pi_1 + \pi_2)\Lambda_h}{\mu_h \mu_c} + \left(P_{c_0} - \frac{(\pi_1 + \pi_2)\Lambda_h}{\mu_h \mu_c}\right) e^{-\mu_c t}.$$
(2.6)

As $t \to \infty$ in (2.6), $P_c \le \frac{(\pi_1 + \pi_1)\Lambda_h}{\mu_h \mu_c}$. Therefore, the feasible solution for the amebiasis pathogen concentration enters the region, $\Pi_2 = \left\{ P_c \in \Re_+ : P_c \leq \frac{(\pi_1 + \pi_1)\Lambda_h}{\mu_h \mu_c} \right\}$. Thus, the feasible region for the model system of equations (2.1) is given by $\Pi = \Pi_1 \times \Pi_2$.

Additionally, given the non-negative parameters of the system described in equation (2.1), it is important to note that the solutions to the system of equations of the amebiasis model are also non-negative. Therefore, it is appropriate to examine the dynamics of the amebiasis model (2.1) within the region $\Pi = \Pi_1 \times \Pi_2$.







IJMSO

Since we are dealing with the human population in relation to living organisms, we need to show that each of the model equations (2.1) is positive. In this regard, we state the following theorem;

Theorem 2.2. The solutions $\left(S_h(t), L_h(t), I_h(t), T_h(t), R_h(t), P_c(t)\right)$ of the system of equations (2.1) are non-negative for all time t > 0 for any given non-negative initial conditions.

Adopting the approach of [22], [35] and Tijani et al [13], we need to show that the solution, $S_h(t)$ is non-negative. Hence, we will prove this using a contradiction. Given that at time, t, $S'_h(t_1) < 0$, $L_h(t_1) > 0$, $I_h(t_1) > 0$, we have

$$S_h'(t_1) = \Lambda_h - \lambda S_h(t_1) + \gamma R_h(t_1) - \mu_h S_h(t_1) = \Lambda_h + \gamma R_h(t_1) > 0,$$

contradicting the assumption that $S'_h(t_1) < 0$. Hence, $S_h(t) > 0$ for t > 0.

Also, for $L_h(t)$, assume \exists a time, t_2 , for $t_1 \neq t_2$, with $L'_h(t_2) < 0$ and all other variables being non-negative at $t \neq t_2$ such that $L_h(t) = 0$. Hence, from the second equation of system (2.1), we get

$$L'_h(t_2) = \lambda S_h(t_2) - (\sigma + \mu_h) L_h(t_2) = \lambda S_h(t_2) > 0$$

. This shows a contradiction to the assumption that $L'_h(t_2) < 0$. Therefore, $L_h(t) > 0$ for t > 0. For $L_h(t)$, assume \exists a time, t_3 , for $t_2 \neq t_3$, with $I'_h(t_3) < 0$ and all other variables being non-negative at $t \neq t_3$ such that $I_h(t) = 0$. Hence, from the third equation of system (2.1),

$$I_h'(t_3) = \sigma L_h(t_3) - (\tau + d_1 + \mu_h)I_h(t_3) = \sigma L_h(t_3) > 0,$$

this contradict the assumption that $I'_h(t_3) < 0$. Hence, $I_h(t) > 0$ for t > 0.

By following the same approach, we can establish that $T_h(t) > 0$, $R_h(t) > 0$, and $P_c(t) > 0$.

This demonstrates that the model is mathematically well-posed and has biological significance, making it a suitable framework for analysing the dynamics of amebiasis.

2.3 Existence of disease-free equilibrium (DFE) and computation of basic reproduction number, R_0

The basic reproduction number, R_0 , is the average number of secondary cases that are reproduced when an infected person is introduced into a totally susceptible population. It is a crucial threshold quantity for infectious disease invasion in the population, implying that $R_0 < 1$ ($R_0 > 1$) means that the disease is eliminated (disease persists) in the population. R_0 is derived using the Nextgeneration matrix [31]. This will be applied in this study as used by [11,12]. We compute R_0 at the disease-free equilibrium, E_0 .

The disease-free equilibrium of the system (2.1), E_0 , is the equilibrium state in the absence of amebiasis disease. Therefore, solving (2.1) at the equilibrium state simultaneously gives the disease-free equilibrium (DFE)

$$E_0 = \left(S_h^0, L_h^0, I_h^0, T_h^0, R_h^0, P_c^0\right) = \left(\frac{\Lambda_h}{\mu_h}, 0, 0, 0, 0, 0, 0\right). \tag{2.7}$$

With apporach of the Next-generation method, we obtain

11(3), 2025, PAGES 138 - 166

HTTPS://DOI.ORG/10.5281/ZENODO.17604865

IJMSO

and

$$V^{-1} = \begin{pmatrix} \frac{1}{f_1} & 0 & 0 & 0\\ \frac{\sigma}{f_1 f_2} & \frac{1}{f_2} & 0 & 0\\ \frac{\tau \sigma}{f_1 f_2 f_3} & \frac{\tau}{f_2 f_3} & \frac{1}{f_3} & 0\\ \frac{\sigma(\tau \pi_2 + \pi_1 f_3)}{f_1 f_2 f_3 \mu_c} & \frac{\sigma(\tau \pi_2 + \pi_1 f_3)}{f_2 f_3 \mu_c} & \frac{\pi_2}{f_3 \mu_c} & \frac{1}{\mu_c} \end{pmatrix},$$

where

$$f_1 = (\sigma + \mu_h), \quad f_2 = (\tau + d_1 + \mu_h), \quad f_3 = (\eta + d_2 + \mu_h), \quad f_4 = (\gamma + \mu_h).$$
 (2.8)

Hence, basic reproduction number, R_0 , which is spectra radius of (FV^{-1}) is given as

$$R_0 = \frac{S^0 \sigma \beta_1 (\alpha \tau + f_3)}{f_1 f_2 f_3} + \frac{S^0 \sigma \beta_2 (\tau \pi_2 + \pi_1 f_3)}{f_1 f_2 f_3 \mu_c}.$$
 (2.9)

Equation (2.9) can be represent as

$$R_0 = R_{0HH} + R_{0EH}$$

where

$$R_{0HH} = \frac{\Lambda_h \sigma \beta_1 (\alpha \tau + (\eta + d_2 + \mu_h))}{\mu_h (\sigma + \mu_h) (\tau + d_1 + \mu_h) (\eta + d_2 + \mu_h)}, R_{0EH} = \frac{\Lambda_h \sigma \beta_2 (\tau \pi_2 + \pi_1 (\eta + d_2 + \mu_h))}{\mu_h (\sigma + \mu_h) (\tau + d_1 + \mu_h) (\eta + d_2 + \mu_h) \mu_c}.$$
(2.10)

This can be further written as

$$R_{0HH_{1}} = \frac{\Lambda_{h}\sigma\beta_{1}\alpha\tau}{\mu_{h}(\sigma + \mu_{h})(\tau + d_{1} + \mu_{h})}, \ R_{0EH_{1}} = \frac{\Lambda_{h}\sigma\beta_{2}\tau\pi_{2}}{\mu_{h}(\sigma + \mu_{h})(\tau + d_{1} + \mu_{h})\mu_{c}}$$

$$R_{0HH_{2}} = \frac{\Lambda_{h}\sigma\beta_{1}}{\mu_{h}(\sigma + \mu_{h})(\tau + d_{1} + \mu_{h})}, \ R_{0EH_{2}} = \frac{\Lambda_{h}\sigma\beta_{2}\pi_{1}}{\mu_{h}(\sigma + \mu_{h})(\tau + d_{1} + \mu_{h})\mu_{c}}.$$
(2.11)

Here, R_{0HH} stands the reproduction number contribution for human-to-human interaction with the transmission rate, β_1 in a total population of size $\frac{\Lambda_h}{\mu_h}$. In contrast, R_{0EH} is the reproduction number contribution of the contaminated environment to human interaction with the transmission rate, β_2 , in a population size $\frac{\Lambda_h}{\mu_h}$.

rate, β_2 , in a population size $\frac{\Lambda_h}{\mu_h}$. It is noteworthy to mention that, R_{0HH} is further split into R_{0HH_1} and R_{0HH_2} , which signifies the contribution for human-to-human interaction for treatment and infected human population while R_{0EH_1} and R_{0EH_2} represents the contribution for environment-to-human interaction for treatment and infected human population through shedding.

2.4 Existence of the endemic equilibrium (EE)

An endemic equilibrium state refers to a condition in which a disease persists within a population. To determine the endemic equilibrium (EE), we set each equation in the system defined by (2.1) to zero. This leads us to derive the expressions from the third, fourth, fifth, and sixth equations of the system (2.1) as follows:

$$L_h = \frac{f_2 I_h}{\sigma}, \quad T_h = \frac{\tau I_h}{f_2}, \quad R_h = \frac{\eta \tau I_h}{f_3 \mu_c}, \quad P_c = \frac{\beta_2 (\pi_1 f_3 + \pi_3 \tau) I_h}{f_3 \mu_c}.$$
 (2.12)

Substituting L_h, T_h , and P_c into second equation of system (2.1), we get for

$$I_h \neq 0, \quad S_h = \frac{f_3 \mu_c f_2 f_1}{\sigma \left[\beta_1 \mu_c (f_3 + \alpha \tau) + \beta_2 (\pi_1 f_3 + \pi_2 \tau) \right]}.$$



Therefore, substituting S_h , L_h , T_h , R_h and P_c into the first equation of system (2.1) yields

$$I_h = \frac{\mu_h f_1 f_2 f_3 \mu_c (R_0 - 1) f_3 f_4}{\left[\beta_1 \mu_c (f_3 + \alpha \tau) + \beta_2 (\pi_1 f_3 + \pi_2 \tau)\right] \left[f_1 f_2 f_3 f_4 + \gamma \eta \tau \sigma\right]}.$$
 (2.13)

Substituting (2.13) in (2.12) to get, L_h, T_h, R_h and P_c , respectively, we have

$$L_{h} = \frac{\mu_{h} f_{1} f_{2}^{2} f_{3} \mu_{c}(R_{0} - 1) f_{3} f_{4}}{\sigma \left[\beta_{1} \mu_{c}(f_{3} + \alpha \tau) + \beta_{2}(\pi_{1} f_{3} + \pi_{2} \tau)\right] \left[f_{1} f_{2} f_{3} f_{4} + \gamma \eta \tau \sigma\right]}.$$

$$T_{h} = \frac{\tau \mu_{h} f_{1} f_{3} \mu_{c}(R_{0} - 1) f_{3} f_{4}}{\left[\beta_{1} \mu_{c}(f_{3} + \alpha \tau) + \beta_{2}(\pi_{1} f_{3} + \pi_{2} \tau)\right] \left[f_{1} f_{2} f_{3} f_{4} + \gamma \eta \tau \sigma\right]}.$$

$$R_{h} = \frac{\eta \tau \mu_{h} f_{1} f_{3}(R_{0} - 1) f_{4}}{\left[\beta_{1} \mu_{c}(f_{3} + \alpha \tau) + \beta_{2}(\pi_{1} f_{3} + \pi_{2} \tau)\right] \left[f_{1} f_{2} f_{3} f_{4} + \gamma \eta \tau \sigma\right]}.$$

$$P_{c} = \frac{\beta_{2}(\pi_{1} f_{3} + \pi_{3} \tau) \mu_{h} f_{1} f_{3}(R_{0} - 1) f_{4}}{\left[\beta_{1} \mu_{c}(f_{3} + \alpha \tau) + \beta_{2}(\pi_{1} f_{3} + \pi_{2} \tau)\right] \left[f_{1} f_{2} f_{3} f_{4} + \gamma \eta \tau \sigma\right]}.$$
(2.16)

$$T_h = \frac{\tau \mu_h f_1 f_3 \mu_c (R_0 - 1) f_3 f_4}{\left[\beta_1 \mu_c (f_3 + \alpha \tau) + \beta_2 (\pi_1 f_3 + \pi_2 \tau)\right] \left[f_1 f_2 f_3 f_4 + \gamma \eta \tau \sigma\right]}.$$
 (2.15)

$$R_h = \frac{\eta \tau \mu_h f_1 f_3 (R_0 - 1) f_4}{\left[\beta_1 \mu_c (f_3 + \alpha \tau) + \beta_2 (\pi_1 f_3 + \pi_2 \tau)\right] \left[f_1 f_2 f_3 f_4 + \gamma \eta \tau \sigma\right]}.$$
 (2.16)

$$P_c = \frac{\beta_2(\pi_1 f_3 + \pi_3 \tau) \mu_h f_1 f_3(R_0 - 1) f_4}{\left[\beta_1 \mu_c(f_3 + \alpha \tau) + \beta_2(\pi_1 f_3 + \pi_2 \tau)\right] \left[f_1 f_2 f_3 f_4 + \gamma \eta \tau \sigma\right]}.$$
 (2.17)

With I_h, L_h, I_h, T_h, R_h and $P_c > 0$ if $R_0 > 1$, it implies that the values of L_h, I_h, T_h, R_h and P_c must be positive. Hence, it indicates that ameliasis disease is said to be endemic whenever $R_0 > 1$.

2.5Stability analysis of the disease-free equilibrium state

Local Stability of the disease-free equilibrium state of the model

The local stability of the disease-free equilibrium point $E_0 = (S_h^0, L_h^0, I_h^0, T_h^0, R_h^0, P_c^0) = (\frac{\Lambda_h}{\mu_h}, 0, 0, 0, 0, 0, 0)$ can be analyzed by examining the linearized form of the equations at the given equilibrium state, E_0 using the theorem below.

Theorem 2.3. The disease-free equilibrium state of the model (2.1) is locally asymptotically stable if $R_0 < 1$ and unstable if $R_0 > 1$.

To determine the local asymptotic stability of the disease-free state, we will employ the linearization method by differentiating each equation in model equations (2.1) with respect to the variables S_h, L_h, I_h, T_h, R_h , and P_c at the disease-crime free equilibrium state and subsequently solve for the eigenvalues. Hence, the Jacobian matrix, $J(E_0)$ is given as follow;

$$J(E_0) = \begin{pmatrix} -\mu_h & 0 & -\beta_1 S_h^0 & -\alpha\beta_1 S_h^0 & \gamma & \beta_2 S_h^0 \\ 0 & -f_1 & \beta_1 S_h^0 & \alpha\beta_1 S_h^0 & 0 & \beta_2 S_h^0 \\ 0 & \sigma & -f_2 & 0 & 0 & 0 \\ 0 & 0 & \tau & -f_3 & 0 & 0 \\ 0 & 0 & 0 & \eta & -f_4 & 0 \\ 0 & 0 & \pi_1 & \pi_2 & 0 & -\mu_c \end{pmatrix}.$$
 (2.18)

Solving for the eigenvalues of matrix (2.18) and using the inspection technique as adopted by [33], we have the first two eigenvalues as $\lambda_1 = -\mu_h$, $\lambda_3 = -f_4$. Therefore, the characteristic equation of the remaining 4×4 matrix of (2.18) is given by

$$\lambda^4 + A\lambda^3 + B\lambda^2 + C\lambda + D = 0, (2.19)$$





IJMSO

where

$$A = (\mu_c + f_3 + f_2 + k_1),$$

$$B = f_1 f_2 (1 - R_{0HH_1}) + f_3 (f_1 + f_2) + \mu_c (f_1 + f_2 + f_3) +,$$

$$C = f_1 f_2 f_3 (1 - R_{0HH}) + f_1 f_2 \mu_c (1 - R_{0HH_1}) + f_1 f_2 (1 - R_{0EH_1}) + f_1 f_3 \mu_c,$$

$$D = f_1 f_2 f_3 \mu_c (1 - R_0).$$
(2.20)

According to [28] as employed by [13], the characteristic equation has all negative real part solutions if the coefficients of the characteristic equation are all positive. Therefore, from the characteristic Equation (2.19), we have A, B, C, D > 0 if $R_{0HH_1}, R_{0EH_1}, R_{0HH} < 1$. Therefore, the Jacobian Matrix, $J(E_0)$ has negative real eigenvalues whenever $R_{0HH_1}, R_{0EH_1}, R_{0HH} < 1$. Thus, the disease-free equilibrium, E_0 , is locally asymptotically stable if $R_0 > 1$. To eliminate the disease, certain conditions must ensure that $R_0 < 1$.

2.5.2Global Stability of the disease-free equilibrium state of the model

With the concept of the Comparison method established [32] as adopted by [11], the E_0 global stability is derived by redrafting the model Equation (2.1) as;

$$\frac{\mathrm{d}X}{\mathrm{d}t} = \Pi(X,Y), \qquad (2.21)$$

$$\frac{\mathrm{d}Y}{\mathrm{d}t} = \Omega(X,Y), \ \Omega(X,0) = 0 \qquad (2.22)$$

$$\frac{\mathrm{d}Y}{\mathrm{d}t} = \Omega(X,Y), \ \Omega(X,0) = 0 \tag{2.22}$$

where $X = (S_h \in \Re^1_+)$ is the sub-class that is disease-free, $Y = (L_h, I_h, T_h, P_c) \in \Re^4_+$ represents the classes that contain the amebiasis disease, which is the sub-classes; humans sub-population and pathogen concentration in the environment that contains the disease. R_h classes are utterly zero without infection in the population.

With X_0 as E_0 , we show that the under listed conditions are satisfied;

$$\Gamma_1$$
: For $\frac{dX}{dt} = \Pi(X_0, 0)$, X_0 is globally asymptotically stable.
 $\Gamma_2: \Omega(X, Y) = AY - \hat{\Omega}(X, Y)$, $\hat{\Omega}(X, Y) > 0$,

where $(X,Y) \in D$ is the region where the model has a feasible solution and as well makes sense epidemiologically, and $A = D_y[\Omega(X_0,0)]$ is an M-matrix resulting from the partial derivative of the infected compartment at DFE. We state the following theorem of stability for the global state at E_0 .

Theorem 2.4. Provide $R_0 < 1$ when there is no disease-related death rate, the disease-free equilibrium state is given as

$$E_0 = \left(S_h^0, L_h^0, I_h^0, T_h^0, R_h^0, P_c^0\right) = \left(\frac{\Lambda_h}{\mu_h}, 0, 0, 0, 0, 0, 0\right)$$

of the model of the system of Eq. (2.1) is globally asymptotically stable, otherwise it is unstable, which implies $R_0 > 1$.

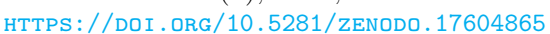
Following the first condition of the Comparison theorem, the disease-free compartment in the sub-model could be presented as

$$\frac{dX}{dt} = (X,0),$$

where

$$\Pi(X,0) = \left(\Lambda_h - \left[\beta_1 (I_h + \alpha T_h) + \beta_2 P_c \right] S_h + \gamma R_h - \mu_h S_h \right).$$







with $X^{\top} = [S_h]$ as the disease-free state variable of the model under consideration, and the disease state variables class $[L_h, I_h, T_h, P_c]$ are all zero. The Jacobian matrix of $\Pi(X, 0)$ is derived as follow

$$\Pi(X,0) = (-\mu_h). \tag{2.23}$$

For the sub-model to be globally asymptotically stable, the eigenvalue of the Jacobian matrix F(X,0) (2.23) must be real and negative. The eigenvalue of the Jacobian matrix F(X,0) (2.23) is $-\mu_h$. This implies that the sub-model under consideration is globally asymptotically stable. For Γ_2 condition, $\Omega(X,Y) = AY - \hat{\Omega}(X,Y)$ with

$$\Omega\left(X,Y\right) = \begin{bmatrix} \left[\beta_{1}(I_{h} + \alpha T_{h}) + \beta_{2}P_{c}\right]S_{h} - (\sigma + \mu_{h})L_{h} \\ \sigma L_{h} - (\tau + d_{1} + \mu_{h})I_{h} \\ \tau I_{h} - (\eta + d_{2} + \mu_{h})T_{h} \\ \pi_{1}I_{h} + \pi_{2}T_{h} - \mu_{c}P_{c} \end{bmatrix}, \quad A = \begin{bmatrix} -f_{1} & \beta_{1}S_{h}^{0} & \alpha\beta_{1}S_{h}^{0} & \beta_{2}S_{h}^{0} \\ \sigma & -f_{2} & 0 & 0 \\ 0 & \tau & -f_{3} & 0 \\ 0 & \pi_{1} & \pi_{2} & -\mu_{c} \end{bmatrix},$$

and

$$\hat{\Omega}(X,Y) = \begin{bmatrix} (S_h^0 - S_h) \Big[\beta_1 I_h + \beta_1 \alpha T_h + \beta_2 P_c \Big] \\ 0 \\ 0 \\ 0 \end{bmatrix}.$$

With this outcome, it is clear that $\hat{\Omega}(X,Y) \geq 0$ since $S_h^0 \geq S_h$.

Thus, $\hat{\Omega}(X,Y) \geq 0$ as $S_h^0 \geq S_h$, this satisfies the two conditions, Γ_1 and Γ_2 . Therefore, the E_0 of the sub-model is globally asymptotically stable if $R_0 < 1$, which implies that the amebiasis disease will be cleared from the population irrespective of the initial sub-populations provided that $R_0 < 1$.

3 Global sensitivity analysis

In this subsection, we conducted a global sensitivity analysis (GSA) to identify the parameters that significantly influence the reproduction number R_0 with multiple points of entry. We utilised the Latin Hypercube Sampling (LHS) method along with the Partial Rank Correlation Coefficient (PRCC) for our analysis. This involved generating 1,000 samples from a uniform distribution within the specified ranges of each parameter, as detailed in the works of [34], [37], [36] and [38]. The parameter values used for the sensitivity analysis are listed in Table 2. The graphical representations of the PRCCs for the parameters affecting R_0 and the results from the 1,000 sampled parameter sets are shown in Figure 2.

As illustrated in Figure 2, the signs (+ and -) of the PRCC indicate a clear qualitative relationship between the parameters and the output of the basic reproduction number, R_0 . Parameters with a positive PRCC suggest that increasing their values will also increase R_0 . Conversely, parameters with negative PRCC values indicate that as their values increase, R_0 decreases. According to Figure 2, R_0 rises as the progression rate from L_h to I_h after the latent period, σ , increases. Additionally, it increases with the shedding rates from T_h to P_c (denoted as π_2), from I_h to P_c (denoted as π_1), as well as with the environment-to-human transmission rate β_2 and the human-to-human transmission rate β_1 . This implies that as these parameters increase, the disease is likely to continue spreading in society. Although π_2 , π_1 , and β_2 have significant effects, other parameters are insignificant based on their monotonicity, with PRCCs < |0.5|. However, the insignificant parameters also tend to influence the spread of the disease.

As the pathogen decay rate (μ_c) , the recovery rate due to treatment (η) , and the progression rate from I_h to T_h due to screening (τ) increase, the basic reproduction number (R_0) decreases. This indicates that as these parameters increase, the disease is more likely to be eliminated from society

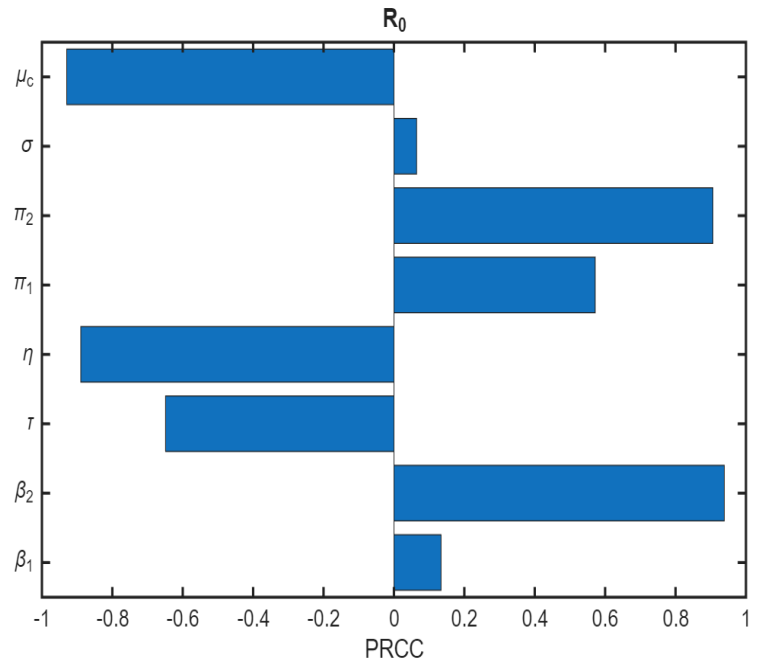


Figure 2: Partial Rank Correlation Coefficient (PRCCs) for important parameters of R_0 .

as they have a more significant impact. It is important to highlight that μ_c and η are the key parameters driving this effect, as their PRCCs $\geq |0.5|$. While other factors can also influence the spread of the disease.

3.1 **Optimal Control Analysis**

In this subsection, we have expanded the basic model of ameliasis from system (2.1) into an optimal control model (3.1), building on the results of the sensitivity analysis. This extension highlighted the need for time-dependent controls, such as:

- u_1 : hygiene practices control,
- u_2 : effective and efficient screening of infected individuals,
- u_3 : efficient and effective treatment control, and
- u_4 : disinfection and sterilisation of the environment control.

The optima control model is given as

$$\frac{dS_{h}}{dt} = \Lambda_{h} - (1 - u_{1}(t)) \left[\beta_{1} (I_{h} + \alpha T_{h}) + \beta_{2} P_{c} \right] S_{h} + \gamma R_{h} - \mu_{h} S_{h},
\frac{dL_{h}}{dt} = (1 - u_{1}(t)) \left[\beta_{1} (I_{h} + \alpha T_{h}) + \beta_{2} P_{c} \right] S_{h} - (\sigma + \mu_{h}) L_{h},
\frac{dI_{h}}{dt} = \sigma L_{h} - \left(\tau (1 + u_{2}(t)) + d_{1} + \mu_{h} \right) I_{h},
\frac{dT_{h}}{dt} = \tau (1 + u_{2}(t)) I_{h} - \left(\eta (1 + u_{3}(t)) + d_{2} + \mu_{h} \right) T_{h},
\frac{dR_{h}}{dt} = \eta (1 + u_{3}(t)) T_{h} - (\gamma + \mu_{h}) R_{h},
\frac{dP_{c}}{dt} = (1 - u_{1}(t)) \pi_{1} I_{h} + (1 - u_{1}(t)) \pi_{2} T_{h} - (1 + u_{4}(t)) \mu_{c} P_{c},$$
(3.1)







with initial conditions of the system (2.1).

The objective function to be minimised is given as

$$J(u_1(t), u_2(t), u_3(t), u_4(t)) = \int_0^{t_f} \left(A_1 I_h + A_2 P_c + \frac{1}{2} \sum_{i=1}^4 m_i u_i^2(t) \right) dt, \tag{3.2}$$

where the coefficient associated with the infected state variables, A, B, and C and the control weight coefficients, m_1, m_2, m_3, m_4 , are assumed positive. The quadratic form of the control variables, $\sum_{i=1}^{4} m_i u_i^2(t)$ in (3.2), is due to the nonlinearity of the cost of controls and as used in the literature on optimal control model of infectious diseases [11, 38, 39].

The objective functional goal is to minimise the number of infected humans, bacteria concentration in the environment and the cost of implementing them. Thus, the optimal controls, $u_1^*(t), u_2^*(t), u_3^*(t), u_4^*(t)$ is sought such that

$$J(u_1^*(t), u_2^*(t), u_3^*(t), u_4^*(t)) = \min_{\Phi_1} J(u_1(t), u_2(t), u_3(t), u_4(t)),$$
(3.3)

where

$$\Phi_1 = \left\{ u_i(t), i = 1, 2, 3, 4 \text{ are measurable with } u_i(t) \in [0, 1], \text{ for } 0 \le t \le t_f \right\}.$$
(3.4)

The state and the control variables of equations (3.2) are non-negative as established in Subsection (3.1), and the condition in Equation (3.4); this implies that the set Φ_1 is closed, convex and exists. The optimal control exists by applying Corollary 4.1 of Pages 68-69 in [42] as implemented in [11,39]. We, therefore, derived the Hamiltonian and optimality system by applying the Pontryagin maximum principle (PMP) [41] to the optimal control problem. PMP transforms Equations (3.1) and (3.2) into a problem of minimizing pointwise Hamiltonian, \mathcal{H} , and it is presented as;

$$\mathcal{H}(S_{h}, L_{h}, I_{h}, T_{h}, R_{h}, P_{c}) = L(I_{h}, P_{c}, u_{1}(t), u_{2}(t), u_{3}(t), u_{4}(t))$$

$$+ \lambda_{1} \frac{dS_{h}}{dt} + \lambda_{2} \frac{dL_{h}}{dt} + \lambda_{3} \frac{dI_{H}}{dt} + \lambda_{4} \frac{dT_{h}}{dt}$$

$$+ \lambda_{5} \frac{dR_{h}}{dt} + \lambda_{6} \frac{dP_{c}}{dt},$$
(3.5)

where $\lambda_1, \lambda_2, \lambda_3, \lambda_4, \lambda_5, \lambda_6$ are the adjoint variables for the respective state variables. Using a similar approach in [11, 12, 39], we derive the following optimality system;

Theorem 4.1. With the optimal control $u_1^*(t), u_2^*(t), u_3^*(t), u_4^*(t)$ and solutions $S_h, L_h, I_h, T_h, R_h, P_c$ that minimizes $J(u_1(t), u_2(t), u_3(t), u_4(t))$ over Φ_1 , there exist non-trivial adjoint functions λ_i , for i = 1, ..., 6 that satisfies;

$$\frac{d\lambda_{1}}{dt} = (\lambda_{1} - \lambda_{2})(1 - u_{1}(t)) \left[\beta_{1}(I_{h} + \alpha T_{h}) + \beta_{2}P_{c}\right] + \lambda_{1}\mu_{h},
\frac{d\lambda_{2}}{dt} = (\lambda_{2} - \lambda_{3})\sigma + \lambda_{2}\mu_{h},
\frac{d\lambda_{3}}{dt} = -A_{1} + (\lambda_{1} - \lambda_{2})(1 - u_{1}(t))\beta_{1}S_{h} + (\lambda_{3} - \lambda_{4})(1 + u_{2}(t))\tau + \lambda_{3}(\mu_{h} + d_{1}) - \lambda_{6}(1 - u_{1}(t))\pi_{1},
\frac{d\lambda_{4}}{dt} = (\lambda_{1} - \lambda_{2})(1 - u_{1}(t))\beta_{1}\alpha S_{h} + (\lambda_{4} - \lambda_{5})(1 + u_{3}(t))\eta + \lambda_{4}(\mu_{h} + d_{2}) - \lambda_{6}(1 - u_{1}(t))\pi_{2},
\frac{d\lambda_{5}}{dt} = (\lambda_{5} - \lambda_{1})\gamma + \lambda_{5}\mu_{h},
\frac{d\lambda_{6}}{dt} = -A_{2} + (\lambda_{2} - \lambda_{1})\beta_{2}(1 - u_{1}(t))S_{h} + \lambda_{6}(1 + u_{4}(t))\mu_{c},$$
(3.6)







HTTPS://DOI.ORG/10.5281/ZENODO.17604865

with the transversality condition $\lambda_i(t_f) = 0$, i = 1, ..., 6 and the controls $u_1^*(t), u_2^*(t), u_3^*(t), u_4^*(t)$ satisfies the optimality condition;

$$\begin{split} u_{1}^{*} &= \max \left\{ 0, \min \left(1, \frac{((\lambda_{2} - \lambda_{1}) \left[\beta_{1} (I_{h} + \alpha T_{h}) + \beta_{2} P_{c} \right] S_{h} + \lambda_{6} (\pi_{1} I_{h} + \pi_{2} T_{h})}{m_{1}} \right) \right\}, \\ u_{2}^{*} &= \max \left\{ 0, \min \left(1, \frac{(\lambda_{3} - \lambda_{4}) \tau I_{h}}{m_{2}} \right) \right\}, \\ u_{3}^{*} &= \max \left\{ 0, \min \left(1, \frac{(\lambda_{4} - \lambda_{5}) \eta T_{h}}{m_{3}} \right) \right\}, \\ u_{4}^{*} &= \max \left\{ 0, \min \left(1, \frac{\lambda_{6} \mu_{c} P_{c}}{m_{4}} \right) \right\}. \end{split}$$
(3.7)

Proof. Using PMP, the adjoint system (3.6) is obtained by differentiating equation (3.5) with respect to their corresponding state variables, $S_h, L_h, I_h, T_h, R_h, P_c$, which is obtained by evaluating the optimal control functions $u_1(t), u_2(t), u_3(t), u_4(t)$ and then applying the negative to the differentials. The optimality condition equation (3.7) is obtained by solving for the controls, $u_1^*(t), u_2^*(t), u_3^*(t), u_4^*(t)$ at the respective steady states;

$$\frac{\partial H}{\partial u_1} = \frac{\partial H}{\partial u_2} = \frac{\partial H}{\partial u_3} = \frac{\partial H}{\partial u_4} = 0$$

on the interior of the control set. Thus, the optimality system comprises Equations (3.6) and (3.7) substituted into (3.1). This ends the proof.

4 Numerical Simulations and Cost-Effectiveness Analysis

4.1 The optimal control problem simulations

The numerical simulation of the optimal control system's outcome is conducted to illustrate the system's dynamics over time. The fourth-order Runge-Kutta method, implemented in MATLAB R2025a, is utilised for these simulations. For details on the fourth-order Runge-Kutta method and its stability, please refer to [11,38]. Table 2 is the parameter values used for the simulations while the initial conditions and weight coefficient values are as follows; $S_h(0) = 100000$, $L_h(0) = 1000$, $I_h(0) = 10$, $I_h(0) =$

The simulations are sectioned into four (4) possible cases according to control combinations; Case A: one control implementation

- Strategy 1 (u_1) : hygiene practices $(u_1 \neq 0, u_2 = u_3 = u_4 = 0)$,
- Strategy 2 (u_2) : effective and efficient screening of some infected humans $(u_2 \neq 0, u_1 = u_3 = u_4 = 0)$,
- Strategy 3 (u_3) : the efficient and effective treatment $(u_3 \neq 0, u_1 = u_2 = u_4 = 0)$,
- Strategy 4 (u_4) : the disinfection/sterilization of the environment control $(u_4 \neq 0, u_1 = u_2 = u_3 = 0)$.

Case B: Two controls combine implementation

• Strategy 5 (u_{12}) : hygiene practices + effective and efficient screening of some infected humans $(u_1, u_2 \neq 0, u_3 = u_4 = 0)$,





- Strategy 6 (u_{13}) : hygiene practices + the efficient and effective treatment $(u_1, u_3 \neq 0, u_2 =$ $u_4 = 0$,
- Strategy 7 (u_{14}) : hygiene practices + the disinfection/sterilization of the environment control $(u_1, u_4 \neq 0, u_2 = u_3 = 0),$
- Strategy 8 (u_{23}) : effective and efficient screening of some infected humans + the efficient and effective treatment $(u_2, u_3 \neq 0, u_1 = u_4 = 0),$
- Strategy 9 (u_{24}) : effective and efficient screening of some infected humans+ the disinfection/sterilization of the environment control $(u_2, u_4 \neq 0, u_1 = u_3 = 0)$,
- Strategy 10 (u₃₄): the efficient and effective treatment +the disinfection/sterilization of the environment control $(u_3, u_4 \neq 0, u_1 = u_2 = 0)$.

Case C: three controls combine implementation

- Strategy 11 (u₁₂₃):hygiene practices + effective and efficient screening of some infected humans + the efficient and effective treatment $(u_1, u_2, u_3 \neq 0, u_4 = 0)$,
- Strategy 12 (u_{124}) : hygiene practices + effective and efficient screening of some infected humans+ the disinfection/sterilization of the environment control $(u_1, u_2, u_4 \neq 0, u_3 = 0)$,
- Strategy 13 (u_{134}) :hygiene practices + the efficient and effective treatment + the disinfection/sterilization of the environment control $(u_1, u_3, u_4 \neq 0, u_2 = 0)$,
- Strategy 14 (u_{234}) : effective and efficient screening of some infected humans + the efficient $u_4 \neq 0, u_1 = 0$).

Case D: all controls combine implementation

• Strategy 15: (u_{1234}) hygiene practices + effective and efficient screening of some infected humans + the efficient and effective treatment + the disinfection/sterilization of the environment control $(u_1, u_2, u_3, u_4 \neq 0)$.

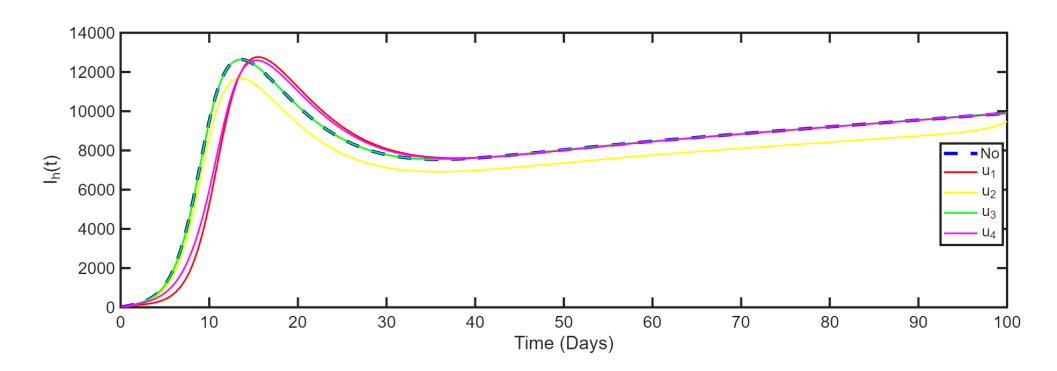


Figure 3: Optimal Control Simulation for Single control on I_h using the parameter values in Table 2.2.

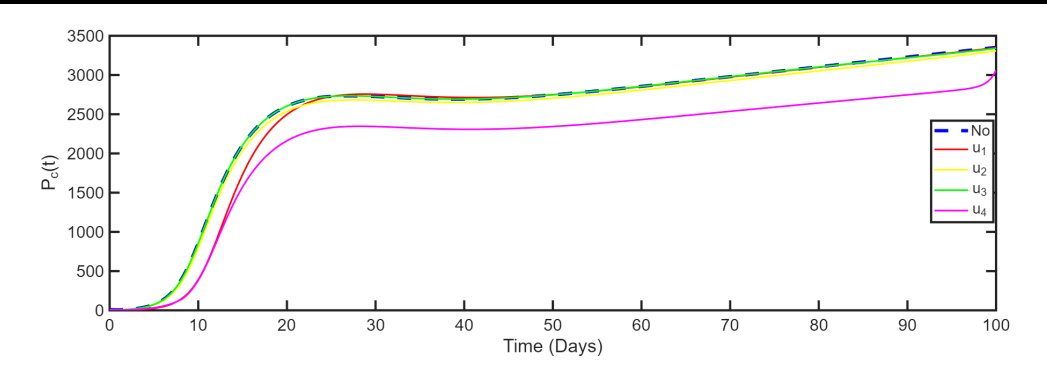


Figure 4: Optimal control simulation for single control on P_c using the parameter values in Table 2.2.

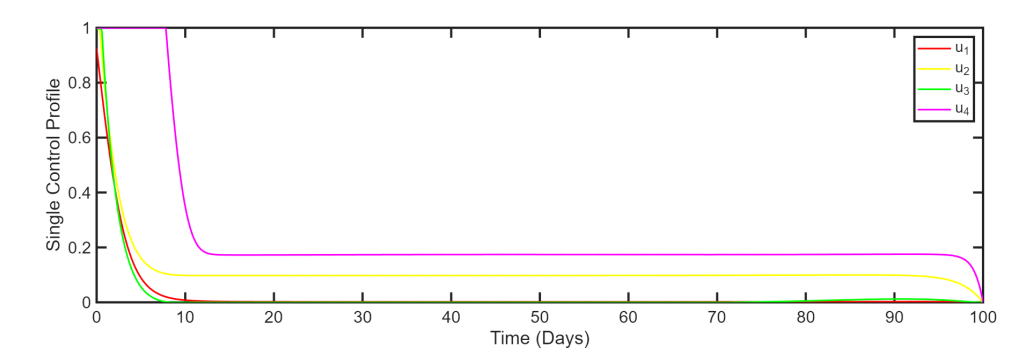


Figure 5: Optimal Control Profile for the Single control strategy using the parameter values in Table 2.2.

Discussion of the optimal control simulation for Case A: Single control imple-4.1.1mentation

Figures 3, 4, and 5 present the results of a single implementation of control measures on infected humans, the concentration of amebiasis in the environment, and the control profile, respectively. In Figure 3, we observed that Strategy 2, which involves effective and efficient screening of infected humans, has the most significant impact on reducing the number of infected individuals, denoted as I_h . This is followed by Strategies 4, 3, and 1 in that order. Although Strategies 4 and 1 do not peak as quickly as the others, by day 60, they become almost insignificant in controlling I_h . Figure 4 shows that Strategy 4, which focuses on the disinfection and sterilisation of the environment, is the most effective at eliminating the amebiasis pathogen in the environment, represented as P_c . This is followed by Strategy 2, which emphasises the effective and efficient screening of some infected individuals, although some remain infectious, particularly after approximately day 30. This finding is consistent with the work of [17] and aligns with the recommendations from [4, 5]. The third figure, 5, illustrates the control profile, highlighting the optimal implementation patterns for each control strategy based on the observed results.

11(3), 2025, PAGES 138 - 166

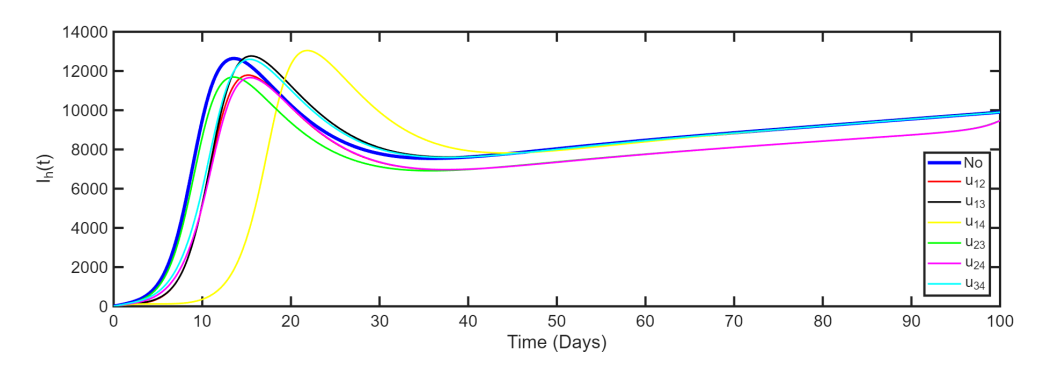


Figure 6: Optimal Control Simulation for Double control on I_h using the parameter values in Table 2.2.

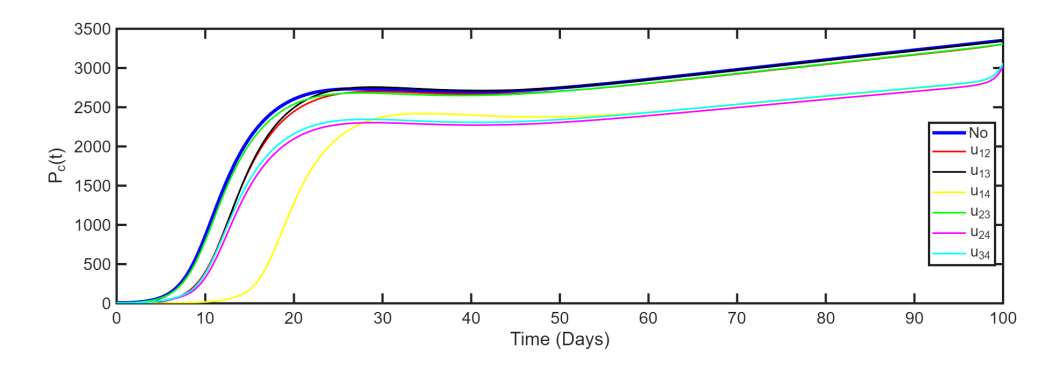


Figure 7: Optimal Control Simulation for Double control on P_c using the parameter values in Table

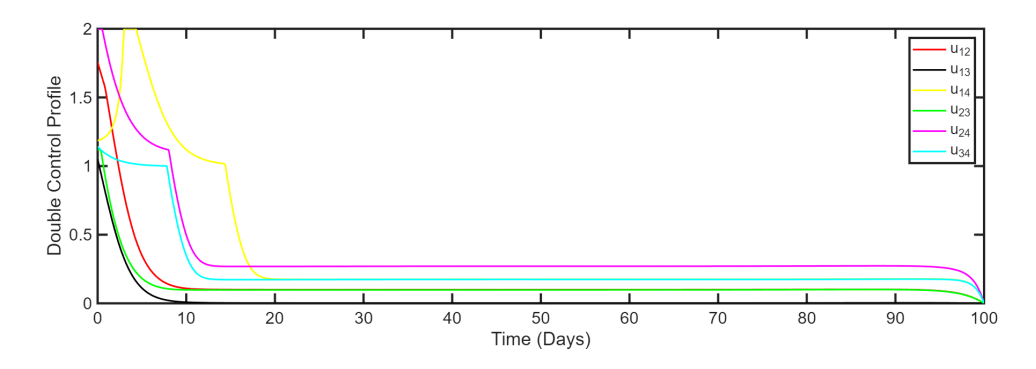


Figure 8: Optimal Control Profile for Double control strategy using the parameter values in Table 2.2.

4.1.2 Discussion of the optimal control simulation for Case B: Double control implementation

Figures 6, 7, and 8 illustrate the results of a dual approach to controlling infected humans, amebiasis concentration in the environment, and the corresponding control profiles. Notably, in Figure 6, Strategy 9, which combines practical and efficient screening of specific infected individuals with disinfection and sterilisation of the environment, has the most significant impact on reducing the



HTTPS://DOI.ORG/10.5281/ZENODO.17604865

number of infected humans, I_h . This is followed by Strategy 8, which involves the effective and efficient screening of infected individuals, along with effective treatment. Although Strategy 7 did not exhibit rapid increases in the early days, it ultimately proved ineffective, similar to Strategies 5, 6, and 10, particularly between days 50 and 100. In Figure 7, Strategy 9 is again the most effective in eliminating the amebiasis pathogen in the environment, denoted as P_c . This is followed by Strategy 7, which incorporates hygiene practices and awareness campaigns along with environmental disinfection and sterilisation. Strategy 10, focusing on efficient and effective treatment, follows next, followed by Strategy 8. This result clearly demonstrates that immediate treatment of individuals who test positive for amebiasis can significantly reduce the spread of amebiasis disease within the population. This finding aligns with the outcomes from [15,17] and supports the recommendations from [2,6]. The optimal implementation patterns for these combinations of controls, based on the results discussed, are presented in Figure 5.

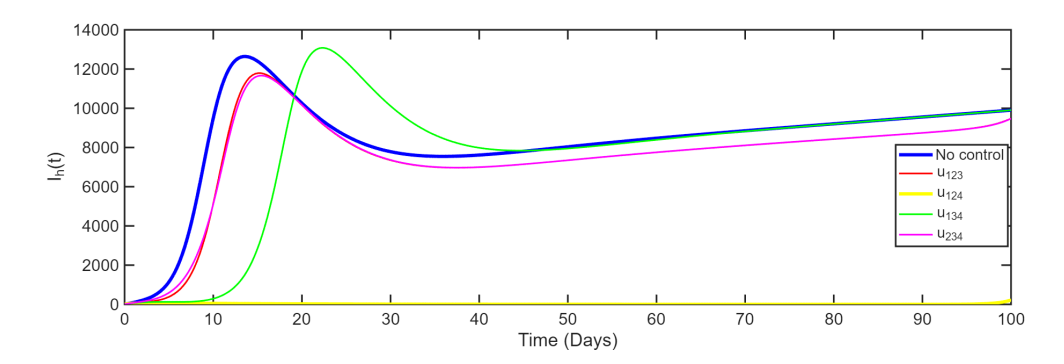


Figure 9: Optimal Control Simulation for Triple control on I_h using the parameter values in Table 2.2.

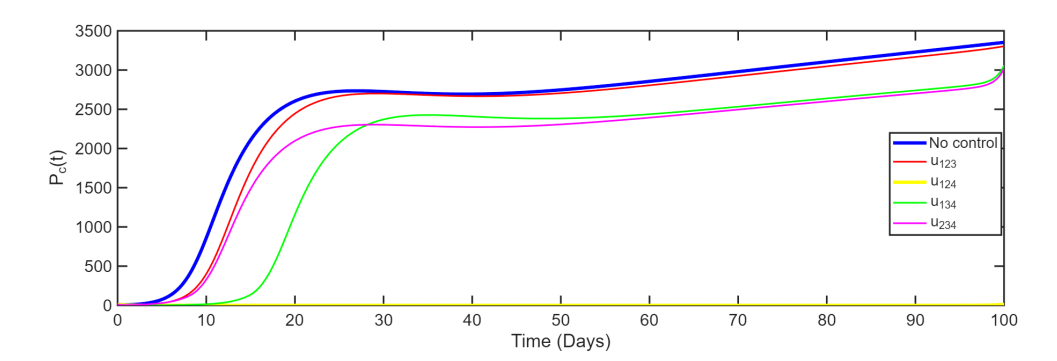


Figure 10: Optimal Control Simulation for Triple control on P_c using the parameter values in Table 2.2.

IJMSO

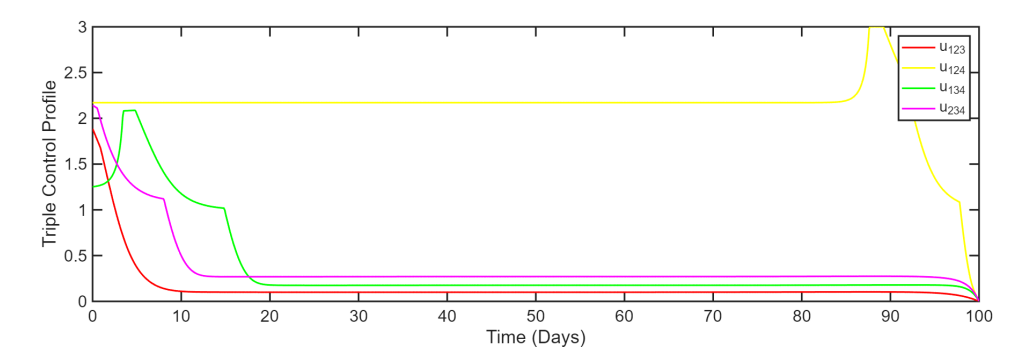


Figure 11: Optimal Control Profile for Triple control strategy using the parameter values in Table 2.2.

4.1.3 Discussion of the optimal control simulation for Case C: Triple control implementation

Figures 9, 10, and 11 illustrate the results of a comprehensive approach to controlling infected humans, pathogen concentration in the environment, and the corresponding control profile. In Figure 9, Strategy 12, which combines hygiene practices, effective screening of infected individuals, and environmental disinfection/sterilisation, emerges as the most significant strategy for reducing the number of infected humans, denoted as I_h . This is followed by Strategy 14, which includes efficient screening of infected individuals, effective treatment, and environmental disinfection/sterilisation. Other strategies prove to be ineffective in comparison to the absence of any control measures. In Figure 10, Strategy 12 again stands out as the most effective approach for eliminating pathogen concentrations in the environment, represented as P_c . This is followed by Strategies 14, 13, and 11, in that order. This conclusion is consistent with the results from [15–17,19] and adheres to the recommendations of [3]. Figure 5 illustrates the recommended implementation patterns for each combination of controls in this triple control strategy.

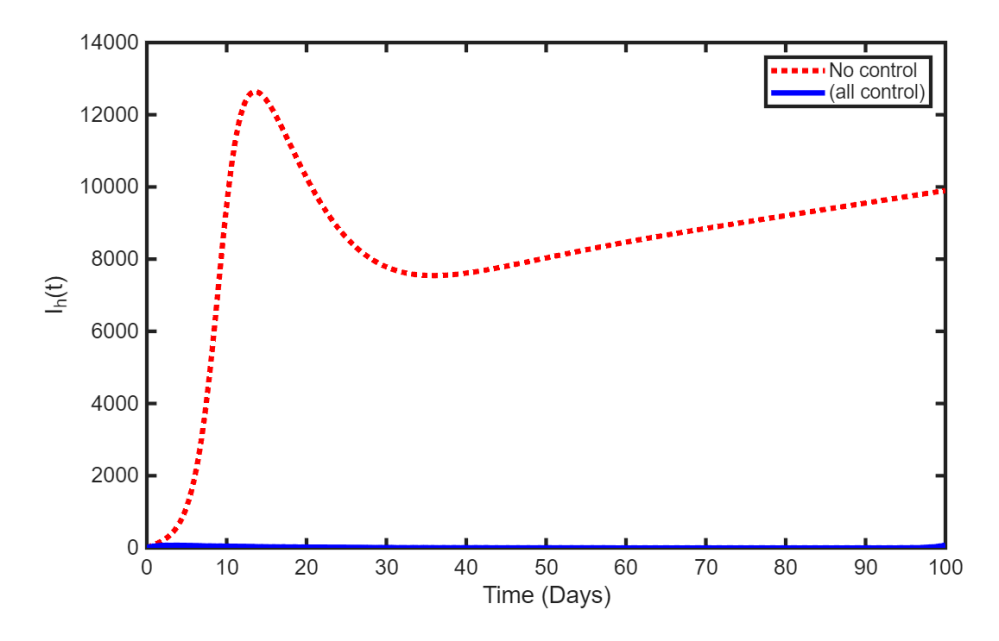


Figure 12: Optimal Control Simulation for Quadruplet (All) control on I_h using the parameter values in Table 2.2.

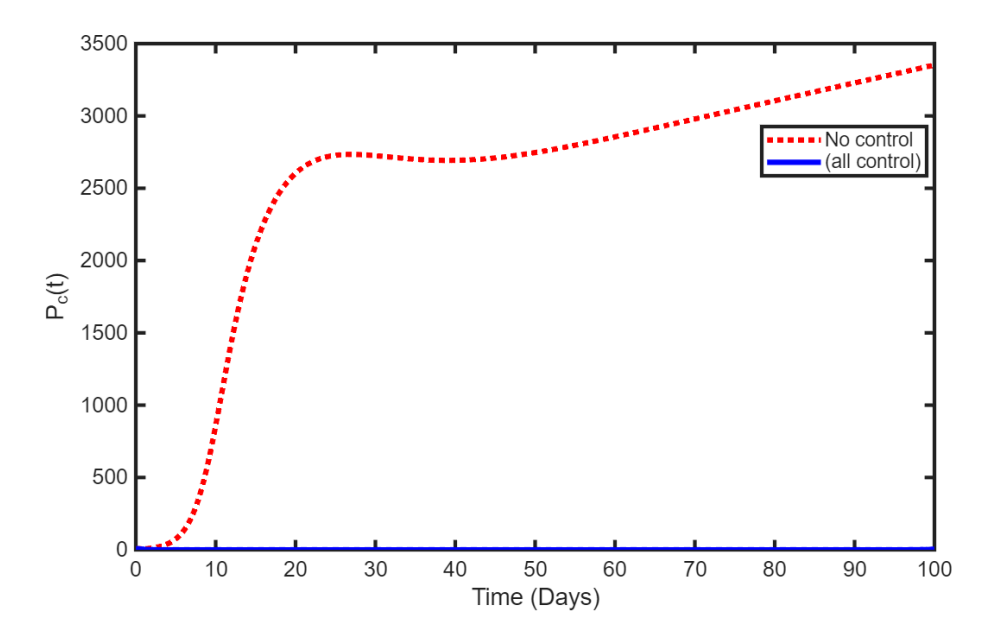


Figure 13: Optimal Control Simulation for Quadruplet (All) control on P_c using the parameter values in Table 2.2.

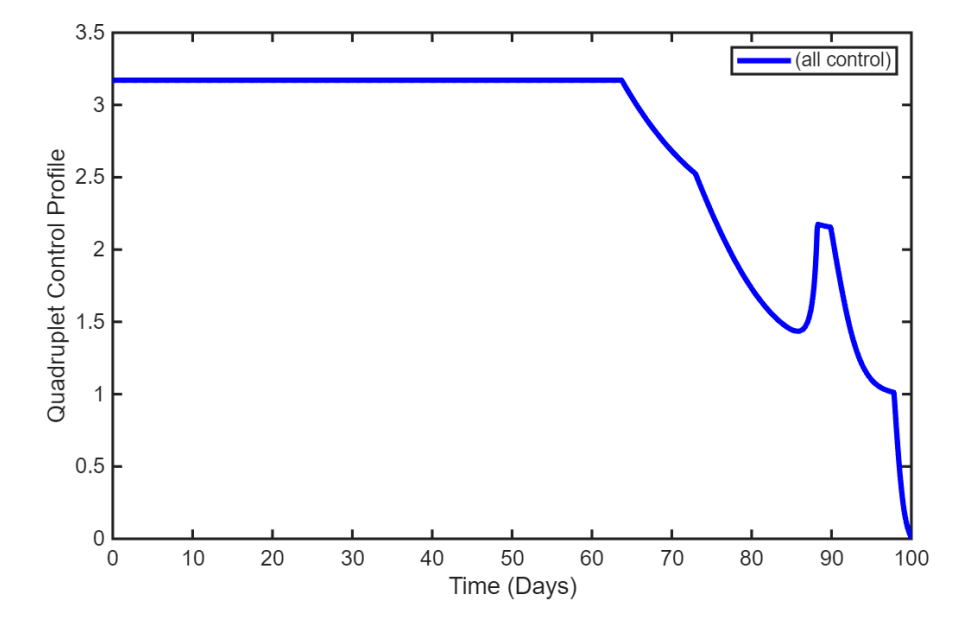


Figure 14: Optimal Control Profile for Quadruplet (All) control strategy using the parameter values in Table 2.2.

4.1.4 Discussion of the optimal control simulation for Case D: Quadruplet control implementation

Figures 12, 13, and 14 illustrate the optimal control simulations for all quadruplet implementations regarding infected humans, pathogen concentration in the environment, and the control profile, respectively. The implementation of all control measures results in the reduction of infected humans,







 I_h , to nearly zero, as shown in Figure 12. Similarly, Figure 13 demonstrates that the pathogen concentration in the environment is also eradicated to almost zero. Figure 14 presents the patterns for implementing all controls as combined control scenarios.

4.2Cost-effectiveness analysis

Cost-effectiveness analysis is a method used to evaluate the costs and economic outcomes associated with one or more control measures. Its purpose is to identify the most cost-effective strategy for eliminating a disease while minimising expenses. In this study, we utilise the incremental costeffectiveness ratio (ICER) as part of our cost-effectiveness analysis methodology [43], [44]].

The incremental cost-effectiveness ratio (ICER) measures the difference in costs and health benefits between two competing intervention strategies that vie for the same limited resources. In the ICER approach, the effectiveness of one strategy is compared to a less effective alternative. The ICER is calculated using the following formula:

When comparing two control intervention strategies, m and n, the Incremental Cost-Effectiveness Ratio (ICER) is calculated as follows:

$$ICER = \frac{Change \ in \ total \ costs \ in \ strategies \ m \ and \ n}{Change \ in \ control \ benefits \ in \ strategies \ m \ and \ n}.$$

The numerator of the Incremental Cost-Effectiveness Ratio (ICER) represents the difference in costs associated with disease infections averted, including expenses related to prevention, disinfection, and screening, among other factors. The denominator of the ICER represents the difference in health outcomes, specifically the total number of infections averted, which is calculated by determining the difference in the total infectious population.

When calculating ICERs, the strategy with the highest ICER value is excluded from consideration, as it represents the most costly and least effective approach. The total infections averted are organised in ascending order in Table 3.

Table 3: Case A (Single control implementation) for Infected cases averted.

Strategy	Infection averted	Total cost	
Strategy 3	153.8670	8.9775	
Strategy 4	1.0229×10^5	5.7721×10^3	
Strategy 1	1.2013×10^5	1.1436×10^{5}	
Strategy 2	6.9810×10^5	1.2241×10^3	

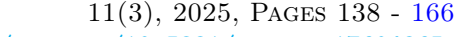
Calculation of ICERs for infected cases averted

ICER for single control implementation for infected cases averted

For Case A, the ICERs are calculated using Table 3 as follows:

$$\begin{split} & \text{ICER}(3) = \frac{8.9775 \, - \, 0}{153.8670 \, - \, 0} = 0.05835, \quad \text{ICER}(4) = \frac{5.7721 \times 10^3 \, - \, 8.9775}{1.0229 \times 10^5 \, - \, 153.8670} = \, 0.05626, \\ & \text{ICER}(1) = \frac{1.1436 \times 10^5 \, - \, 5.7721 \times 10^3}{1.2013 \times 10^5 \, - \, 1.0229 \times 10^5} = 6.08677, \; \text{ICER}(2) = \frac{1.2241 \times 10^3 \, - \, 1.1436 \times 10^5}{6.9810 \times 10^5 \, - \, 1.2013 \times 10^5} = -0.19575. \end{split}$$

The computed results indicate that the ICER value for Strategy 1, denoted as ICER (1), significantly dominates the other strategies. This means that the implementation of u_1 is more costly and less effective compared to the strategies based on u_2 , u_3 , and u_4 . Therefore, Strategy 1 is removed from the list of alternative control strategies. As a next step, we will calculate the ICERs for u₂,







HTTPS://DOI.ORG/10.5281/ZENODO.17604865

 u_3 , and u_4 in ascending order based on the total number of infections averted. This yields

$$ICER(3) = \frac{8.9775 - 0}{153.8670 - 0} = 0.05835, \quad ICER(4) = \frac{5.7721 \times 10^3 - 8.9775}{1.0229 \times 10^5 - 153.8670} = 0.05626,$$

$$ICER(2) = \frac{1.2241 \times 10^3 - 5.7721 \times 10^3}{6.9810 \times 10^5 - 1.0229 \times 10^5} = -0.007635.$$

Based on the computed outcomes, the ICER for Strategy 3 is higher than that of Strategies 4 and 2. This indicates that Strategy 3 will be removed from the list of alternative control strategies. Therefore, we will calculate the ICERs for u_4 and u_2 in ascending order of the total number of infections averted as

$$ICER(4) = \frac{5.7721 \times 10^3 - 0}{1.0229 \times 10^5 - 0} = 0.05643, \ ICER(2) = \frac{1.2241 \times 10^3 - 5.7721 \times 10^3}{6.9810 \times 10^5 - 1.0229 \times 10^5} = -0.007635.$$

Since the ICER of Strategy 4 is significantly higher than that of Strategy 2, it indicates that Strategy 4 is more expensive and less effective. Consequently, Strategy 4 has been removed from the list of alternative control interventions. As a result, Strategy 2, which focuses on the effective and efficient screening of some infected individuals (u_2) , is considered the most cost-effective optimal control strategy for combating the bacterial disease. This is followed by Strategy 4, which involves the disinfection and sterilisation of the environment (u_4) , as illustrated in Figures 3 and 4.

The total infections averted for the double control combination are organised in ascending order in Table 4.

Table 4: Case B (Double control implementation) for Infected cases averted.

Strategy	Infection averted	Total cost	
Strategy 10	1.0227×10^5	5.7836×10^3	
Strategy 6	1.2126×10^5	1.1626×10^5	
Strategy 7	5.1609×10^{5}	6.0626×10^5	
Strategy 8	6.9778×10^{5}	1.2379×10^{3}	
Strategy 9	7.9137×10^5	7.3213×10^3	
Strategy 5	7.9447×10^5	8.0299×10^4	

ICER for double control implementation for infected cases averted

The ICER for Case B is calculated as follows using Table 4;

$$\begin{split} & \text{ICER}(10) = \frac{5.7836 \times 10^3 \, - \, 0}{1.0227 \times 10^5 \, - \, 0} = 0.0566, \quad \text{ICER}(6) = \frac{1.1626 \times 10^5 \, - \, 5.7836 \times 10^3}{1.2126 \times 10^5 \, - \, 1.0227 \times 10^5} = 5.8144, \\ & \text{ICER}(7) = \frac{6.0626 \times 10^5 \, - \, 1.1626 \times 10^5}{5.1609 \times 10^5 \, - \, 1.2126 \times 10^5} = 1.2411, \quad \text{ICER}(8) = \frac{1.2379 \times 10^3 \, - \, 6.0626 \times 10^5}{6.9778 \times 10^5 \, - \, 5.1609 \times 10^5} = -3.3299, \end{split}$$

$$ICER(9) = \frac{7.3213 \times 10^3 - 1.2379 \times 10^3}{7.9137 \times 10^5 - 6.9778 \times 10^5} = 0.0650, \ ICER(5) = \frac{8.0299 \times 10^4 - 7.3213 \times 10^3}{7.9447 \times 10^5 - 7.9137 \times 10^5} = 23.541.$$

The results indicate that the ICER for Strategy 5 is greater than those of the other strategies in Case B. Therefore, Strategy 5 has been removed from the list of substitute intervention strategies. We will now calculate the ICERs for the remaining strategies—10, 6, 7, 8, and 9—arranging them in ascending order based on the total number of infections averted. This is given as

$$ICER(10) = \frac{5.7836 \times 10^{3} - 0}{1.0227 \times 10^{5} - 0} = 0.0566, \quad ICER(6) = \frac{1.1626 \times 10^{5} - 5.7836 \times 10^{3}}{1.2126 \times 10^{5} - 1.0227 \times 10^{5}} = 5.8144,$$

$$ICER(7) = \frac{6.0626 \times 10^{5} - 1.1626 \times 10^{5}}{5.1609 \times 10^{5} - 1.2126 \times 10^{5}} = 1.2411, \quad ICER(8) = \frac{1.2379 \times 10^{3} - 6.0626 \times 10^{5}}{6.9778 \times 10^{5} - 5.1609 \times 10^{5}} = -3.3299,$$

ICER(9) =
$$\frac{7.3213 \times 10^3 - 1.2379 \times 10^3}{7.9137 \times 10^5 - 6.9778 \times 10^5} = 0.0650.$$

The ICER for Strategy 6 is higher than that of the other strategies, indicating that it is more expensive than the competing options. Consequently, we will exclude Strategy 6 from the list of alternative interventions for Case B. We will then calculate the ICERs for the remaining strategies,

presented in ascending order based on the number of infections averted. gives this
$$ICER(10) = \frac{5.7836 \times 10^3 - 0}{1.0227 \times 10^5 - 0} = 0.0566, \quad ICER(7) = \frac{6.0626 \times 10^5 - 5.7836 \times 10^3}{5.1609 \times 10^5 - 1.0227 \times 10^5} = 1.4511,$$

$$ICER(8) = \frac{1.2379 \times 10^3 - 6.0626 \times 10^5}{6.9778 \times 10^5 - 5.1609 \times 10^5} = -3.3299, \quad ICER(9) = \frac{7.3213 \times 10^3 - 1.2379 \times 10^3}{7.9137 \times 10^5 - 6.9778 \times 10^5} = 0.0650.$$

Based on the calculations, Strategy 7 is more costly and less effective. Therefore, it has been removed from the list of control intervention options. We will now compute the ICERs for the remaining three strategies, arranging them in ascending order by the number of infections averted. This gives

$$\begin{split} & \text{ICER}(10) = \frac{5.7836 \times 10^3 \, - \, 0}{1.0227 \times 10^5 \, - \, 0} = 0.0566, \ \ \text{ICER}(8) = \frac{1.2379 \times 10^3 \, - \, 5.7836 \times 10^3}{6.9778 \times 10^5 \, - \, 1.0227 \times 10^5} = -0.00763, \\ & \text{ICER}(9) = \frac{7.3213 \times 10^3 \, - \, 1.2379 \times 10^3}{7.9137 \times 10^5 \, - \, 6.9778 \times 10^5} = 0.0650. \end{split}$$

Strategy 9 has an ICER higher than the other strategies, indicating that it is strongly dominated; it is both more expensive and less effective. As a result, Strategy 9 is eliminated from consideration among the alternative control strategies. We will then evaluate the ICERs of the remaining two strategies in order of the number of infections averted, as outlined below:

$$ICER(10) = \frac{5.7836 \times 10^3 - 0}{1.0227 \times 10^5 - 0} = 0.0566, \quad ICER(8) = \frac{1.2379 \times 10^3 - 5.7836 \times 10^3}{6.9778 \times 10^5 - 1.0227 \times 10^5} = -0.00763.$$

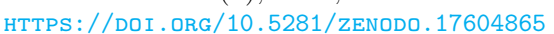
The results indicate that the ICER of Strategy 10 is higher than that of Strategy 8, making it more expensive and less effective. Consequently, Strategy 10 has been eliminated from consideration. The remaining viable option is Strategy 8. This strategy, which combines effective and efficient screening of infected individuals with efficient and effective treatment (u_{23}) , is identified as the most cost-effective approach for disease containment in the context of double control implementation. This is illustrated graphically in Figures 6 and 7.

Table 5: Case C (Triple control implementation) for Infected cases averted.

Strategy	Infection averted	Total cost	
Strategy 13	5.4639×10^5	6.5441×10^5	
Strategy 14	7.9142×10^5	7.3394×10^{3}	
Strategy 11	7.9477×10^5	8.0797×10^4	
Strategy 12	8.3212×10^{6}	9.1281×10^{6}	

ICER for triple control implementation for infected cases averted







The ICER for Case C is calculated as follows using the details in Table 5;

$$\begin{split} & \text{ICER}(13) = \frac{6.5441 \times 10^5 - 0}{5.4639 \times 10^5 - 0} = 1.1977, \quad \text{ICER}(14) = \frac{7.3394 \times 10^3 - 6.5441 \times 10^5}{7.9142 \times 10^5 - 5.4639 \times 10^5} = -2.6408, \\ & \text{ICER}(11) = \frac{8.0797 \times 10^4 - 7.3394 \times 10^3}{7.9477 \times 10^5 - 7.9142 \times 10^5} = 21.9276, \quad \text{ICER}(12) = \frac{9.1281 \times 10^6 - 8.0797 \times 10^4}{8.3212 \times 10^6 - 7.9477 \times 10^5} = 1.2021. \end{split}$$

The calculations indicate that the ICER for Strategy 11 is both more expensive and less effective. Consequently, it is removed from the list of alternative control strategies for Case C. Next, we calculate the ICERs for the remaining three strategies, organising them in ascending order based on the number of infections they have averted, as follows:

$$\begin{split} & \text{ICER}(13) = \frac{6.5441 \times 10^5 - 0}{5.4639 \times 10^5 - 0} = 1.1977, \quad & \text{ICER}(14) = \frac{7.3394 \times 10^3 - 6.5441 \times 10^5}{7.9142 \times 10^5 - 5.4639 \times 10^5} = -2.6408, \\ & \text{ICER}(12) = \frac{9.1281 \times 10^6 - 7.3394 \times 10^3}{8.3212 \times 10^6 - 7.9142 \times 10^5} = 1.2113. \end{split}$$

The results indicate that Strategy 12 has a higher ICER than the other two strategies, meaning it is both more expensive and less effective. As a result, Strategy 12 is eliminated from the list of competing intervention strategies. We will now calculate the ICERs for the remaining two strategies, in order of the number of infections averted, starting with the one that yields the lowest. This is given as

$$ICER(13) = \frac{6.5441 \times 10^5 - 0}{5.4639 \times 10^5 - 0} = 1.1977, \quad ICER(14) = \frac{7.3394 \times 10^3 - 6.5441 \times 10^5}{7.9142 \times 10^5 - 5.4639 \times 10^5} = -2.6408.$$

The results indicate that the ICER for Strategy 13 is greater than that of Strategy 14, which implies that Strategy 13 is more costly and less effective. Consequently, Strategy 14, which combines efficient and effective screening of infected individuals, effective treatment, and environmental disinfection and sterilisation (denoted as u_{234}), emerges as the most cost-effective triple-combined control strategy for combating amebiasis disease in Case C. Following closely is Strategy 13, which integrates hygiene practices and awareness campaigns with efficient treatment and environmental disinfection (denoted as u_{134}). This information is illustrated graphically in Figures 9 and 10.

Table 6: The most Cost-Effective Strategy of each Case in ascending Order of Total Infections Averted.

Strategy	Infection averted	Total cost	
Strategy 8	6.9778×10^5	1.2379×10^3	
Strategy 2	6.9810×10^5	1.2241×10^3	
Strategy 14	7.9142×10^5	7.3394×10^3	
Strategy 15	3.9656×10^{6}	1.1159×10^{7}	

Calculation of overall ICER for infection cases averted

We present the overall total infection averted and their respective total cost in Table 6. The information is used to calculate the overall ICERs for the most cost-effective strategies in Cases A, B, and C, as well as Case D. The computation is given as follows:

$$ICER(8) = \frac{1.2379 \times 10^3 - 0}{6.9778 \times 10^5 - 0} = 0.001774, \ ICER(2) = \frac{1.2241 \times 10^3 - 1.2379 \times 10^3}{6.9810 \times 10^5 - 6.9778 \times 10^5} = -0.04313,$$

International Journal of Mathematical Sciences and OPTIMIZATION: THEORY AND APPLICATIONS 11(3), 2025, PAGES 138 - 166

HTTPS://DOI.ORG/10.5281/ZENODO.17604865

$$ICER(14) = \frac{7.3394 \times 10^3 - 1.2241 \times 10^3}{7.9142 \times 10^5 - 6.9810 \times 10^5} = 0.0655, ICER(15) = \frac{1.1159 \times 10^7 - 7.3394 \times 10^3}{3.9656 \times 10^6 - 7.9142 \times 10^5} = 3.51324.$$

Based on these results, Strategy 15 has a higher ICER than the other three strategies (8, 2, 14). This indicates that Strategy 15 is costly and not very effective, leading to its elimination from the list of alternative control intervention strategies. Consequently, we will compute the ICERs of the remaining two strategies in ascending order based on the total number of infections averted. This is presented as follows:

$$\begin{split} & \text{ICER}(8) = \frac{1.2379 \times 10^3 \, - \, 0}{6.9778 \times 10^5 \, - \, 0} = 0.001774, \ \ \text{ICER}(2) = \frac{1.2241 \times 10^3 \, - \, 1.2379 \times 10^3}{6.9810 \times 10^5 \, - \, 6.9778 \times 10^5} = -0.04313, \\ & \text{ICER}(14) = \frac{7.3394 \times 10^3 \, - \, 1.2241 \times 10^3}{7.9142 \times 10^5 \, - \, 6.9810 \times 10^5} = 0.0655. \end{split}$$

Based on the results, Strategy 14 has a higher ICER compared to the other two strategies, indicating that it is less effective and more costly. Therefore, Strategy 14 has been removed from the list of alternative control intervention strategies. The ICERs of the remaining two strategies will be calculated in order of the total infections averted, as shown below:

$$ICER(8) = \frac{1.2379 \times 10^3 - 0}{6.9778 \times 10^5 - 0} = 0.001774, \ ICER(2) = \frac{1.2241 \times 10^3 - 1.2379 \times 10^3}{6.9810 \times 10^5 - 6.9778 \times 10^5} = -0.04313.$$

Strategy 8, which combines effective and efficient screening of some infected individuals with efficient treatment, has a greater ICER than Strategy 2. This indicates that Strategy 8 is both more expensive and less effective. As a result, it has been removed from the list of control strategy options. Therefore, Strategy 2, which focuses on effective and efficient screening of some infected individuals, is identified as the most cost-effective strategy for containing the amebiasis parasite.

Conclusion 5

In this paper, we present a nonlinear deterministic mathematical model formulated using ordinary differential equations to study the dynamics of amebiasis. We established the invariant region, ensured the positivity of solutions, and identified the steady states of the system. To calculate the basic reproduction number, R_0 , we employed the next-generation method.

We analysed the local and global stability of the disease-free equilibrium (DFE) and found that it is asymptotically stable both locally and globally when $R_0 < 1$ and unstable when $R_0 > 1$. Additionally, we conducted a global sensitivity analysis using LHS in conjunction with the PRCC to identify the most sensitive parameters influencing the spread of the disease.

Following the sensitivity analysis results, we proposed an optimal control model that incorporates four time-dependent interventions to combat the spread of amebiasis disease. These interventions are: Hygiene practices (control variable u_1), Effective and efficient screening of infected individuals (control variable u_2), Efficient and effective treatment of infected individuals (control variable u_3), and Disinfection and sterilisation of the environment (control variable u_4). supports these interventions citeBarwell, Shirley. The model is analysed using the Pontryagin Maximum Principle, with numerical simulations conducted for the infected human population, represented as $I_h(t)$, and the concentration of the ameliasis pathogen in the environment, denoted as $P_c(t)$. The analysis includes four different cases: A, B, C, and D.

The results from the optimal control simulations are used to conduct a cost-effectiveness analysis based on the Incremental Cost-Effectiveness Ratio (ICER). The findings indicate that any combination of controls, including effective and efficient screening of infected individuals, is the most cost-effective strategy for reducing amebiasis within the community. If sufficient resources are available, all four controls can be implemented simultaneously. However, when resources are limited, the most cost-effective approach for Case A (single control) is the efficient screening of a subset



International Journal of Mathematical Sciences and Optimization: Theory and Applications $11(3),\,2025,\,{\rm Pages}\,\,138$ - 166

HTTPS://DOI.ORG/10.5281/ZENODO.17604865

of infected individuals, denoted as u_2 . In the case of a double combined control strategy, when additional resources are available, Strategy 8—which includes both effective screening of infected individuals and efficient treatment, represented as u_{23} —is identified as the most effective in eradicating the disease. For Case C, which involves a triple control strategy with ample resources, the most cost-effective option is Strategy 14. This strategy combines practical screening of infected individuals, efficient treatment, and environmental disinfection/sterilisation, represented as u_{234} .

Overall, the most cost-effective strategy identified is Strategy 2, which focuses solely on the effective and efficient screening of a subset of infected individuals (u_2) . This indicates that when individuals infected with amebiasis are screened and confirmed, it leads to immediate treatment, which can cure the disease and reduce its transmission dynamics, either directly or indirectly. This conclusion aligns with the findings of [17] and resonates with the recommendations made by [4, 5].

The limitations of this study include the derivation of stability for the endemic equilibrium and the application of real-world data, both of which will be addressed in future research.

6 Data availability

All the Data (parameter values) used in this work have been cited appropriately in Table2

Acknowledgement

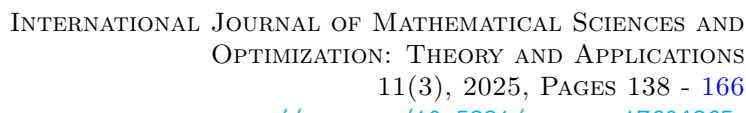
The authors express their sincere gratitude to the International Mathematical Union (IMU) for the financial support as one of the beneficiaries of Graduate Assistantships grant in Developing Countries..

References

- [1] Barwell, J. Amebiasis. (2023). Accessed from https://www.healthline.com/health/amebiasis
- [2] Shirley, D.A.T., Farr, L., Watanabe, K. and Moonah, S. A Review of the Global Burden, New Diagnostics, and Current Therapeutics for Amebiasis. (2018). Open Forum Infect. Dis. 2018;5:ofy161. doi: 10.1093/ofid/ofy161
- [3] CDC. Amebiasis. (2025). Accessed from https://www.cdc.gov/amebiasis/about/index.html
- [4] Cleveland Clinic Amebiasis (Amoebic Dysentery). (2022) Accessed from https://my.clevelandclinic.org/health/diseases/23531-amoebic-dysentery
- [5] Carrero, J. C., Reyes-López, M., Serrano-Luna, J., Shibayama, M., Unzueta, J., León-Sicairos, N. and De La Garza, M. Intestinal Amoebiasis: 160 Years of Its First Detection and Still Remains as a Health Problem in Developing Countries. Int. J. Med. Microbiol. 2020;310:151358. doi: 10.1016/j.ijmm.2019.151358.
- [6] Ikbal, A., Debnath, B., Rajkhowa, A., Paul, K., Majumder, R. and Manna, K. (2022). Amoebiasis: An Infectious Disease Caused by Entamoeba histolytica. Asian Journal of Basic Science & Research. 04. 32-40. 10.38177/AJBSR.2022.4202.
- [7] Ximénez, C., Morán, P., Rojas, L., Valadez, A.and Gómez, A. Reassessment of the Epidemiology of Amebiasis: State of the Art.(2009). Infect. Genet. Evol. 2009;9:1023–1032. doi: 10.1016/j.meegid.2009.06.008.
- [8] Samie, A., ElBakri, A. and AbuOdeh, R. E. Amoebiasis in the tropics: Epidemiology and pathogenesis. (2012). Curr Top Trop Med, 201 (2012)



- Zaman, G., Jung, I. H., Torres, F. M. D. & Zeb, A.. (2017) "Mathematical Modelling and Control of Infectious Disease", Computational and Mathematical Method in Medicine, 7149154. https://doi.org/10.1155/2017/7149154.
- [10] Gweryina, R. I., Madubueze, C. E. & Kaduna, F. S. (2021). Mathematical Assessment of the Role of Denial on COVID-19 Transmission with N n-Linear Incidence and Treatment Functions. Sci Afr. 12:e00811. doi: 10.1016/j.sciaf.2021.e00811. Epub 021 Jun 14. PMID: 34151051; PMCID: PMC8200329.
- [11] Odeh, J. O., Agbata, B. C., Tijani, K. A. & Madubueze, C. E.(2024). Optimal Control Strategies for the Transmission Dynamics of Zika Virus: With the Aid of Wolbachia-Infected Mosquitoes. *Numerical and Computational Methods in Sciences and Engineering.* **5**(1), 2024,PP: 1-25, doi:10.18576/ncmse/050101.
- [12] Tijani, K. A., Madubueze, C. E. & Gweryina, R.I. (2024). Modelling Typhoid Fever Transmission with Treatment Relapse Response: Optimal Control and Cost-Effectiveness Analysis. *Math Models Comput Simul* **16**2024, 457–485 . https://doi.org/10.1134/S2070048224700169.
- [13] Kazeem A. Tijani, Chinwendu. E. Madubueze, Isaac O. Onwubuya, Nkiruka Maria-Assumpta Akabuike and John Olajide Akanni. (2025). Mathematical modelling of the dynamical system of military population, focusing on the impact of welfare, *J. Nig. Soc. Phys. Sci.*, 7 (2025) 2844, DOI:10.46481/jnsps.2025.2844.
- [14] Hategekimana, F., Saha, S., and Chaturvedi, A. (2017). Dynamics of Amoebiasis Transmission: Stability and Sensitivity Analysis. Mathematics, 5(4), 58. https://doi.org/10.3390/math5040058
- [15] Edward, S. and Mpogolo, G. E. Modeling and optimal control of the transmission dynamics of amebiasis. (2023).Results in Control and Optimization, Volume 13, 2023, 100325, ISSN 2666-7207, https://doi.org/10.1016/j.rico.2023.100325.
- [16] Mpeshe, S. C. Fuzzy SEIR Epidemic Model of Amoebiasis Infection in Human. (2022). Advance in Fuzzy Systems. https://doi.org/10.1155/2022/5292830
- [17] Fidele, H., Chaturvedi, A., Snehanshu, S. and Kigali, R. Modeling The Dynamics of Amoebiasis Transmission: Case of Simultaneous Infectious States. Accessed from https://www.researchgate.net/profile/Snehanshu-Saha/publication/335223231_Modeling_The_Dynamics_of_Amoebiasis_Transmission_Case_of_Simultaneous_Infectious_States/links/5d59953392851cb74c75fea1/Modeling-The-Dynamics-of-Amoebiasis\protect\discretionary{\char\hyphenchar\font}{}}Transmission-Case-of-Simultaneous-Infectious-States.pdf
- [18] Hategekimana, F., Saha, S.,& Chaturvedi, A. (2016). Amoebiasis Transmission and Life cycle: A continuous state description by virtue of existence and uniqueness. Global Journal of Pure and Applied Mathematics, 12(1), 375-390.
- [19] Mwaijande, S. E. and Mpogolo, G. E. (2022). Mathematical Modeling of The Transmission Dynamics of Amoebiasis With Some Interventions, 03 March 2022, PREPRINT (Version 1) available at Research Square [https://doi.org/10.21203/rs.3.rs-1363033/v1]
- [20] Birkhoff, G and Rota, G. (1969). Ordinary Differential Equations, 2nd ed., Waltham, Mass.: Blaisdell Publishing Co.
- [21] Tijani, K. A., Madubueze, C. E. & Gweryina, R. I. (2023). Typhoid fever dynamical model with cost-effective optimalcontrol. *Journal of the Nigerian Society of Physical Sciences*, **5**(4),2023, 1579. https://doi.org/10.46481/jnsps.2023.1579





HTTPS://DOI.ORG/10.5281/ZENODO.17604865

- [22] Madueme, P, U and Chirove, F. (2023). Understanding the transmission pathways of Lassa fever: A mathematical modeling approach. Infectious Disease Modelling, 8(2023); 27-57.https://doi.org/10.1016/j.idm.2022.11.010.
- [23] Stauffer, W. and Ravdin, J.I: Entamoeba histolytica: an update. Current opinion in infectious diseases, 16(5), 479-485(2003).
- [24] Tilahum, G. T., Oluwole, D. M. & David, M.. (2017). "Modelling and Optimal Control of Ty-phoid Fever Disease with Cost Effective Strategies", Computationa and Mathematical methods in Medicine, 2324518 (2017). https://doi.org/10.1155/2017
- [25] Encyclopedia of Mathematics, "Optimal control, mathematical theory of", (2020). Accessed on http://encyclopediaofmath.org/index.php?title=Optimal_control,_mathematical_theory_of&oldid=48051
- [26] Lauer, J. A. Morton, A. & Bertram, M. (2019). "Cost-Effectiveness Analysis", in Ole F. Norheim, Ezekiel J. Emanuel, and Joseph Millum (eds), Global Health Priority-Setting: Beyond Cost-Effectiveness (New York, 2019; online edn, Oxford Academic, 19 Dec. 2019), https://doi.org/10.1093/oso/9780190912765.003.0005, accessed 23 Apr. 2023.
- [27] Heymann, D. L., Ed., Control of Communicable Diseases Manual, American Public Health Association, Washington DC, USA, 20 edition, 2015.
- [28] Heffernan, J. M., Smith, R. J. & Wahl, L. M. Perspectives on the Basic Reproductive Ratio. Journal of the Royal Society Interface. 2(2005): 281-293.
- [29] Keeling, Matt J., and Pejman Rohani. Modeling infectious diseases in humans and animals. Princeton university press, 2011.
- [30] Davis, C. P. and Balentine, J. R. (2019). "Amebiasis (Entamoeba histolytica infection)," 2019, https://www.medicinenet.com/amebiasis_entamoeba_histolytica_infection/article.htm
- [31] Van den Driessche P. and Watmough, J. (2002). Reproduction Number and Subthreshold Endemic Equilibrium for Compartmental Models of Disease Transmission. *Mathematical Biosciences*, 2002:29-48
- [32] Castillo-Chavez, C., Feng, Z. and Huang, W. (2002) On the Computation of RO and Its Role on Global Stability. In: Castillo-Chavez, P.C., Blower, S., Driessche, P., Kirschner, D. and Yakubu, A.-A., Eds., Mathematical Approaches for Emerging and Reemerging Infectious Diseases: An Introduction, Springer, Berlin, 229.
- [33] Lunga, M. M, (2012). Mathematical Models for the coinfection Dynamics of Cholera and Ty-phoid (Doctoral Thesis/Master's Dissertation). Johannesburg: University of Johannesbur. Avail- able from: http://hdl.hnadle.net/102000/0002(Accessed on 20 June, 2024)
- [34] Blower, S. M. & Dowlatabadi, H. (1994). Sensitivity and Uncertainty Analysis of Complex Models of Disease Transmissio: an HIV Model, as an Example. *International Statistical Re*view, 62(1994): 229-243.
- [35] Odetunde, O., & Ibrahim, M. O. (2021). Stability Analysis of Mathematical Model of a RelapseTuberculosis Incorporating Vaccination. *International Journal of Mathematical Sciences and Optimization: Theory and Applications*, 7(1), 116-130.
- [36] Danbaba, U. A., Aloko, M. D., & Ayinde, A. M. (2024). Mathematical modeling of mosquito borne diseases with vertical transmissions as applied to Dengue. *International Journal of Mathematical Sciences and Optimization: Theory and Applications*, 10(3), 31 56. Retrieved from https://ijmso.unilag.edu.ng/article/view/2195



International Journal of Mathematical Sciences and Optimization: Theory and Applications 11(3), 2025, Pages 138 - 166

HTTPS://DOI.ORG/10.5281/ZENODO.17604865

- [37] Marino, S., Hogue, I. B., Ray, C. J. & Kirschner, D. E.(2008) A Methodology for Performing Global Uncertainty and Sensitivity Analysis in S stems Biology. *Journal of Theoretical Biology.* **254**(1), 2008: 178-196.
- [38] Madubueze, C. E. Tijani, K. A. & Fatmawati. (2023) A deterministic mathematical model for optimal control of diphtheria disease with booster vaccination. *Healthcare Analytics*, 4(2023),100281, ISSN 2772-4425,https://doi.org/10.1016/j.health.2023.100281.
- [39] Gweryina, R. I., Madubueze, C. E., Baijya, V. P. & Esla, F. E. (2023). "Modeling and Analysis of Tuberculosis and Pneumonia Co-Infection Dynamics with Cost-Effective Strategies". *Results in Control and Optimization*, **10**(2023): 100210.
- [40] Akanni, J. O., Akinpeli, F. O. & Ogunsola, A. W. "Modelling Financial Crime Population Dynamics: Optimal Control and Cost-Effectiveness Analysis", International Journal of Dynamics and Control, 8(2020), 531-544.
- [41] Pontryagin, L. S., Boltyanskii, V. G., Gamkrelidze, R. V. and Mishchenko, E. F. "The Mathematical Theory of Optimal Processes", John Wiley & Sons, London, UK (1962).
- [42] Fleming, W. A., and Rishel, R. W. "Deterministic and Stochastic Optimal Control", Springer Verlag, New York (1975).
- [43] Asamoah, J. K. K., Okyere, E., Abidemi, A., Moore, S. E., Sun, G., Jim, Z., Acheampong, E. & Gordon, J. F. (2022). "Optimal Control and Comprehensive Cost Effectiveness for Covid 19", Results in Physics, 33(2022) 105177. https://doi.org/10.1016/j.rinp.2022.105177
- [44] Berhe, H. W., Makinde, O. D. & Thevri, D. M.. (2007). "Optimal Control and Cost-Effectiveness Analysis for Dysentery Epidemic Model", International Journal of Applied Mathematics and Information Sciences, 12(6), 1183-1195 (2007). https://doi.org/10.18576/amis/120613